Steroid receptor coactivators 1 and 2 mediate fetal-to-maternal signaling that initiates parturition

Lu Gao,[1,2] Elizabeth H. Rabbitt,[1] Jennifer C. Condon,[1] Nora E. Renthal,[1] John M. Johnston,[1] Matthew A. Mitsche,[3] Pierre Chambon,[4] Jianming Xu,[5] Bert W. O'Malley,[5] and Carole R. Mendelson[1,6]

[1]Department of Biochemistry, University of Texas Southwestern Medical Center, Dallas, Texas, USA. [2]Department of Physiology, Second Military Medical University, Shanghai, China. [3]Department of Molecular Genetics, University of Texas Southwestern Medical Center, Dallas, Texas, USA. [4]Department of Physiological Genetics and Molecular Biology, Institut de Génétique et de Biologie Moléculaire et Cellulaire, University of Strasbourg Institute for Advanced Study, and Collège de France, Illkirch, France. [5]Department of Molecular and Cellular Biology, Baylor College of Medicine, Houston, Texas, USA. [6]Department of Obstetrics and Gynecology, University of Texas Southwestern Medical Center, Dallas, Texas, USA.

The precise mechanisms that lead to parturition are incompletely defined. Surfactant protein-A (SP-A), which is secreted by fetal lungs into amniotic fluid (AF) near term, likely provides a signal for parturition; however, SP-A–deficient mice have only a relatively modest delay (~12 hours) in parturition, suggesting additional factors. Here, we evaluated the contribution of steroid receptor coactivators 1 and 2 (SRC-1 and SRC-2), which upregulate SP-A transcription, to the parturition process. As mice lacking both SRC-1 and SRC-2 die at birth due to respiratory distress, we crossed double-heterozygous males and females. Parturition was severely delayed (~38 hours) in heterozygous dams harboring SRC-1/-2–deficient embryos. These mothers exhibited decreased myometrial NF-κB activation, $PGF_2\alpha$, and expression of contraction-associated genes; impaired luteolysis; and elevated circulating progesterone. These manifestations also occurred in WT females bearing SRC-1/-2 double-deficient embryos, indicating that a fetal-specific defect delayed labor. SP-A, as well as the enzyme lysophosphatidylcholine acyltransferase-1 (LPCAT1), required for synthesis of surfactant dipalmitoylphosphatidylcholine, and the proinflammatory glycerophospholipid platelet-activating factor (PAF) were markedly reduced in SRC-1/-2–deficient fetal lungs near term. Injection of PAF or SP-A into AF at 17.5 days post coitum enhanced uterine NF-κB activation and contractile gene expression, promoted luteolysis, and rescued delayed parturition in SRC-1/-2–deficient embryo-bearing dams. These findings reveal that fetal lungs produce signals to initiate labor when mature and that SRC-1/-2–dependent production of SP-A and PAF is crucial for this process.

Introduction

Preterm birth is a leading cause of neonatal morbidity and mortality worldwide (1–4). Globally, approximately 15 million babies are born prematurely each year (1) and approximately 1.1 million babies die annually from complications of prematurity (4). The initiation of labor, both at term and preterm, is associated with an upregulated inflammatory response, exemplified by increased proinflammatory cytokines in amniotic fluid (AF) (5); infiltration of myometrium, cervix, and fetal membranes by neutrophils and macrophages (6–8); and a decline in progesterone (P_4) receptor (PR) function. In preterm labor, intraamniotic (i.a.) infection likely provides a prominent stimulus for increased AF cytokines and inflammatory cell migration (9, 10). However, the precise signals for the inflammatory response leading to labor at term remain unclear (11).

Parturition timing in all species appears to be mediated by signals from both mother and fetus (11). Near term, increased uterine stretch (12, 13) and factors produced by the developing fetus (6, 14–16) may provide inflammatory stimuli. Previously, we (6) and others (17) suggested that the fetus may provide a signal via pulmonary surfactant, a developmentally regulated, glycerophospholipid-rich lipoprotein produced by pulmonary alveolar type II cells and secreted into AF in increased amounts during late gestation (11). Surfactant, which reduces surface tension within the lung alveoli after birth, is essential for air breathing. Thus, infants born prematurely are at risk of developing respiratory distress syndrome because of surfactant deficiency. We further suggested that the major surfactant protein, surfactant protein-A (SP-A), a C-type lectin also secreted by the fetal lungs into AF near term, could serve as a hormonal signal for parturition (6). SP-A stimulated IL-1β expression in cultured AF macrophages, and i.a. injection of SP-A caused preterm delivery of fetuses within 6 to 24 hours (6). In mice, targeted deletion of the genes encoding SP-A and the related C-type lectin, SP-D, caused a modest but significant parturition delay and prevented induction of "contractile" genes, oxytocin receptor (*Oxtr*) and connexin-43 (*Cx43*, also known as gap junction protein 1 [*Gja1*]), in myometrium (15). While these findings were compelling, both parents were double KO (dKO) for *SP-A* and *SP-D*. Thus, a role for fetal signaling was not definitively proven. Moreover, the parturition delay was observed only in the second or subsequent pregnancies, suggesting a requirement for other signals.

Our previous studies revealed that a 300-bp region upstream of the *SP-A* gene mediates its developmental, tissue-specific, and

▶ Related Commentary: p. 2569

Conflict of interest: The authors have declared that no conflict of interest exists.
Submitted: August 20, 2014; **Accepted:** May 6, 2015.
Reference information: *J Clin Invest*. 2015;125(7):2808–2824. doi:10.1172/JCI78544.

hormonal regulation of expression (18, 19). Steroid receptor coactivators 1 and 2, SRC-1 and SRC-2, serve important roles in transcriptional upregulation of *SP-A* gene expression in fetal lung type II cells (20, 21). Endogenous SRC-1 in human fetal lung (HFL) type II cells was recruited with thyroid transcription factor-1 (TTF-1, also known as Nkx2.1) and NF-κB to the *hSP-A* promoter upon cAMP and IL-1 stimulation of *SP-A* expression (21, 22). cAMP also enhanced estrogen-related receptor α (ERRα) transcriptional activity at the *SP-A* promoter by increasing its interaction with protein kinase A and SRC-2 (20).

SRCs belong to the p160 coactivator family, comprised of three homologous members: SRC-1 (also known as ERAP140, ERAP160, and NCOA1), SRC-2 (also known as TIF-2, GRIP-1, and NCOA2), and SRC-3 (also known as p/CIP, RAC3, AIB1, TRAM-1, and ACTR). Although they do not directly bind to DNA, coactivators can robustly increase the transcriptional activities of nuclear receptors and other transcription factors by bridging them to factors bound to other response elements and to the basal transcription machinery and by recruiting other coregulators (23, 24). Through recruitment of coregulators causing posttranslational modification of histones, they can alter chromatin structure, resulting in transcriptional activation or repression (25).

Studies using KO mice indicate that, although structurally similar, each SRC family member has specific physiological functions (24). For example, although *SRC-1*$^{-/-}$ mice are fertile, female mice manifest reduced estrogen-stimulated uterine growth and decreased P_4-dependent uterine decidual response (26). Male *SRC-2*$^{-/-}$ mice are infertile due to defects in spermatogenesis (27), while female *SRC-2*$^{-/-}$ mice display placental hypoplasia and hypofertility (28). In light of our previous findings that SRC-1 and SRC-2 serve roles in the regulation of *SP-A* gene expression, we were intrigued by the finding that mice lacking both *SRC-1* and *SRC-2* (*SRC-1*$^{-/-}$ *SRC-2*$^{-/-}$ mice, herein referred to as *SRC-1/-2* dKO mice) died at birth of respiratory distress (29), suggesting a deficiency of pulmonary surfactant production.

To investigate the molecular basis for effects of SRC-1 and SRC-2 on surfactant synthesis by the fetal lung, we analyzed SRC-1 and SRC-2 double-deficient mice. Unexpectedly, we uncovered a pathway that we believe to be novel by which SRC-1 and SRC-2 coordinately control pregnancy length and the initiation of labor through their impact on production of surfactant lipid and proteins by the fetal lung.

Results

SRC-1/SRC-2 double deficiency in mice results in delayed labor. To define the phenotypic consequences of deficiency in SRC-1 and SRC-2, we crossed male and female mice that were double heterozygous for *SRC-1* and *SRC-2* (*SRC-1*$^{+/-}$ *SRC-2*$^{+/-}$ mice, herein referred to as *SRC-1/-2* dhet mice). To ensure that parturition timing was analyzed in mice of the same physiological status, only data from first pregnancies were included. Surprisingly, out of 49 *SRC-1/-2* dhet crosses, only 8 mice delivered at term (19.5 days post coitum [dpc]). The majority of the pregnant mice (~84%) delivered 1 to 2 days late or had to be sacrificed at 22.5 dpc because of a failure to deliver spontaneously (Figure 1A). Thus, a pronounced and statistically significant delay in the time to parturition was observed in *SRC-1/-2* dhet females bred to genotypically matched males (20.89 ± 0.13 dpc; $n = 49$) ($P < 0.001$) compared with that in their WT C57BL/6 (B6) counterparts (19.42 ± 0.08; $n = 13$) (Figure 1B). Notably, when bred to genotypically matched males, no difference in the time to labor was evident among *SRC-1*$^{-/-}$ (19.44 ± 0.07 dpc; $n = 16$) or *SRC-2*$^{+/-}$ (19.50 ± 0.0 dpc; $n = 10$) females, compared with that in WT B6 controls (Figure 1B). More interestingly, a similar significant delay in parturition timing was observed in WT female mice bred to *SRC-1*$^{-/-}$ *SRC-2*$^{+/-}$ (herein referred to as 1-KO/2-het) male mice (20.94 ± 0.22 dpc; $n = 25$) ($P < 0.001$) compared with that in WT B6 mice (Figure 1B), suggesting that the defect causing the delay in labor initiation is fetal in origin.

To assess whether the observed delays in parturition were associated with defects in fecundity, we compared litter size among WT female mice bred to 1-KO/2-het or to WT male mice and *SRC-1/-2* dhet female mice bred to *SRC-1/-2* dhet male mice during first pregnancies. We found the average litter size across all genotypes to be similar (Supplemental Table 1; supplemental material available online with this article; doi:10.1172/JCI78544DS1). Notably, *SRC-1/-2* dhet females bred to genotypically matched males or WT females bred to 1-KO/2-het males manifested a similar delayed labor during second and subsequent pregnancies (Supplemental Table 2).

The litters generated from *SRC-1/-2* dhet female mice bred to *SRC-1/-2* dhet male mice are expected to be comprised of 9 possible genotypes according to Mendelian law (Figure 1A). Upon genotyping all of the fetuses in each litter, we plotted the proportion of *SRC-1 SRC-2* double-deficient pups (which included *SRC-1/-2* dhet, *SRC-1/-2* dKO, 1-KO/2-het, *SRC-1*$^{+/-}$ *SRC-2*$^{-/-}$ pups [herein referred to as 1-het/2-KO pups]) for each of the crosses relative to gestational length. A strongly positive correlation was found between the proportion of *SRC-1 SRC-2* double-deficient pups in corresponding litters and the timing of parturition (Figure 1C).

SP-A synthesis and secretion are impaired in fetal lungs of SRC-1/-2–deficient mice. In light of the evidence that the delayed-labor phenotype was caused by an alteration in signals produced by SRC-1/-2–deficient fetuses, as well as our previous findings that SRC-1 and SRC-2 are important for transcriptional regulation of *SP-A* in fetal lung type II cells (20, 21), we analyzed the *SP-A* mRNA and protein expression in fetal lungs and secretion of SP-A protein into AF. Notably, *SP-A* mRNA and protein in lungs of *SRC-1/-2* double-deficient fetuses were significantly decreased compared with those of WT fetuses and with those of fetuses that were singly deficient in SRC-1 or SRC-2 (Figure 1, D and E). Moreover, SP-A protein in AF of *SRC-1/-2* double-deficient fetuses also was dramatically decreased compared with that of WT fetuses and with that of fetuses that were singly deficient for either coactivator (Figure 1F).

To determine whether other surfactant proteins were affected by *SRC-1/-2* deficiency, we analyzed expression of SP-D, a C-type lectin structurally similar to SP-A, as well as the hydrophobic surfactant protein, SP-B, which is essential for air breathing (30, 31). Expression of these two surfactant proteins was unaffected in lung tissues of *SRC-1/-2* double-deficient fetal mice (Supplemental Figure 1, A and B). Additionally, the ATP-binding cassette, subfamily A, member 3 (ABCA3), an essential transporter that mediates surfactant lipoprotein trafficking and lamellar body biogenesis (32, 33), showed only modest, nonsignificant changes in lungs of *SRC-1/-2* double-deficient fetuses (Supplemental Figure 1C).

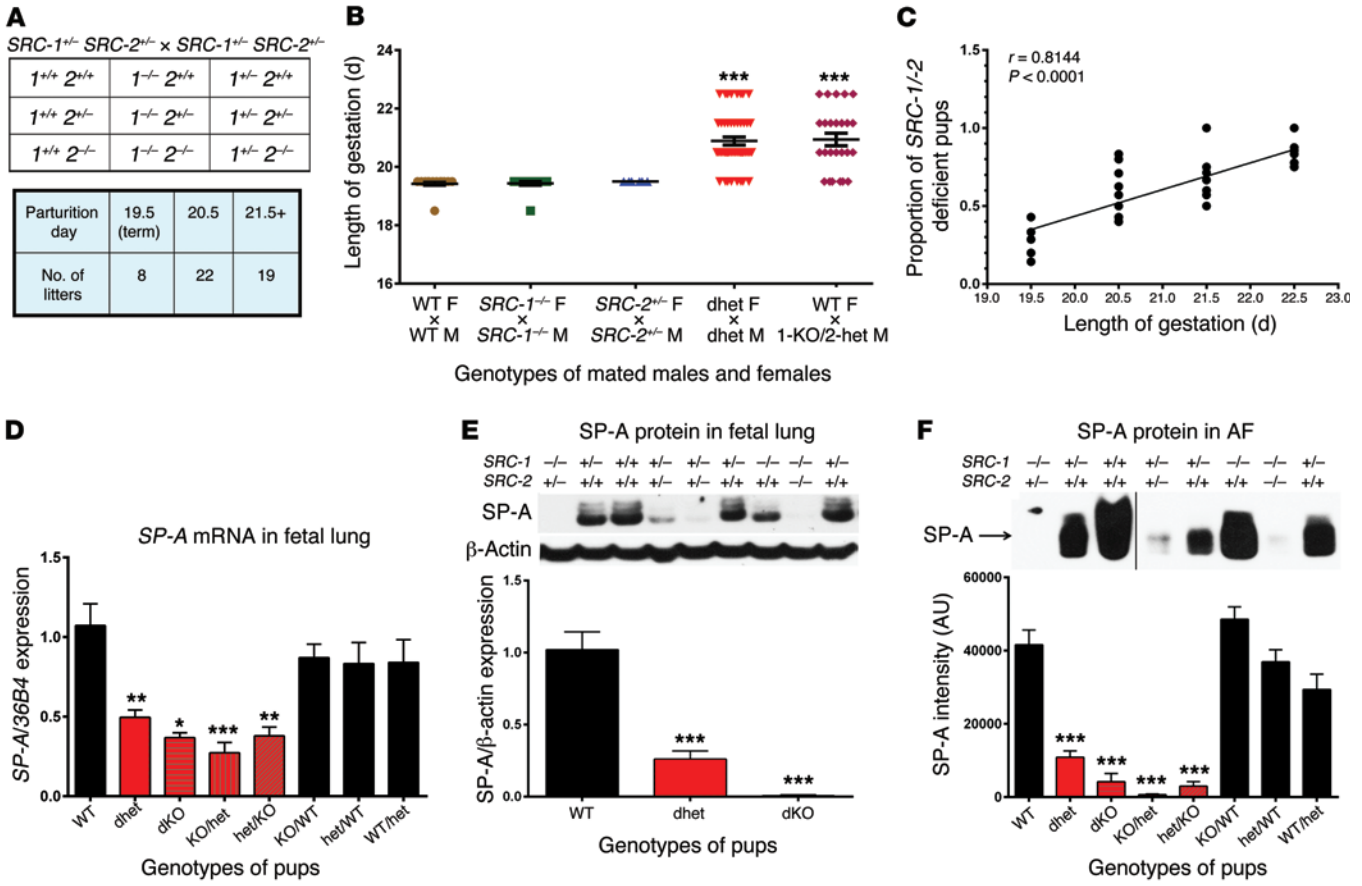

Figure 1. Delayed parturition in *SRC-1/-2* dhet female × *SRC-1/-2* dhet male and WT female × 1-KO/2-het male is associated with reduced SP-A expression in lungs of *SRC-1/-2* double-deficient fetuses. (**A**) Genotypes resulting from crosses of *SRC-1/2* dhet females × *SRC-1/2* dhet males and gestation length of pregnancies resulting from these double heterozygous crosses. (**B**) Gestation length of WT females × WT males (n = 13), *SRC-1*$^{-/-}$ females × *SRC-1*$^{-/-}$ males (n = 16), *SRC-2*$^{+/-}$ females × *SRC-2*$^{+/-}$ males (n = 10), *SRC-1/-2* dhet females × *SRC-1/-2* dhet males (n = 49), and WT females × 1-KO/2-het males (n = 25). (**C**) Gestation length of *SRC-1/-2* dhet females × *SRC-1/-2* dhet males is positively correlated with proportion of *SRC-1 SRC-2* double-deficient pups. (**D**) *SP-A* mRNA in lungs of WT (n = 4), *SRC-1/-2* dhet (dhet; n = 14), *SRC-1/-2* dKO (dKO; n = 3), 1-KO/2-het (KO/het; n = 6), *SRC-1* het/*SRC-2* KO (het/KO; n = 6), *SRC-1* KO/*SRC-2* WT (KO/WT; n = 3), *SRC-1* het/*SRC-2* WT (het/WT; n = 13), and *SRC-1* WT/*SRC-2* het (WT/het; n = 4) fetuses at 18.5 dpc from matings of *SRC-1/-2* dhet females × *SRC-1/-2* dhet males. (**E**) SP-A protein in 18.5 dpc fetal lung from *SRC-1/-2* dhet females × *SRC-1/-2* dhet males. Representative immunoblot of SP-A protein according to genotype, and data from scans of SP-A immunoblots normalized to β-actin for WT (n = 6), *SRC-1/-2* dhet (n = 6), and *SRC-1/-2* dKO (n = 4) fetuses. (**F**) SP-A protein in AF surrounding WT and *SRC-1/-2*–deficient fetuses. In the representative immunoblot, the first 3 lanes were run on same gel but were noncontiguous with the remaining 5 lanes (divided by the black line). Combined data from scans of immunoblots of SP-A in AF surrounding WT (n = 5), dhet (n = 14), dKO (n = 3), KO/het (n = 6), het/KO (n = 6), KO/WT (n = 3), het/WT (n = 13), and WT/het (n = 4) fetuses. Data are mean ± SEM. *P < 0.05, **P < 0.01, ***P < 0.001 (ANOVA).

To confirm the KO efficiencies of SRC-1 and SRC-2 in fetal lungs, we performed real-time PCR and found that *SRC-1* and *SRC-2* mRNA were essentially undetectable in *SRC-1* KO fetal lungs and *SRC-2 KO* fetal lungs, respectively. Neither was detected in *SRC-1/-2* dKO fetal lungs. Interestingly, *SRC-1* mRNA expression was markedly and significantly increased in fetal lungs of *SRC-2* KO mice, while *SRC-2* mRNA was significantly increased in fetal lungs of *SRC-1* KO mice (Supplemental Figure 1, D and E, respectively), suggesting that SRC-1 and SRC-2 are upregulated in a compensatory manner in vivo.

NF-κB activation is decreased in myometrium of WT or SRC-1/-2–deficient females bred to SRC-1/-2–deficient males. We previously suggested that the developmental increase in SP-A expression in mouse fetal lung and its secretion into the AF after 17 dpc can activate AF macrophages via binding to TLR2. The activated macrophages, in turn, may transit to the maternal uterus, resulting in increased cytokine production and myometrial NF-κB activation (6, 15). To determine whether a deficiency of SRC-1/-2 affected the activation of inflammatory signaling pathways, the proinflammatory transcription factors, NF-κB p65 and p50, were analyzed in myometrial cytoplasmic and nuclear fractions by immunoblotting. Notably, nuclear levels of NF-κB p65 and p50 proteins were greatly reduced in myometrial tissues of *SRC-1/-2* dhet or WT females bred to *SRC-1/-2* double-deficient males relative to WT crosses at 18.5 dpc, in association with a coordinate increase in cytoplasmic levels of these proteins (Figure 2, A and B). These findings suggest that inflammatory stimuli promoting nuclear translocation and activation of NF-κB were impaired in the pregnant uterus near term, in association with the decrease in SP-A expression and secretion in *SRC-1/-2*–deficient fetal mice.

Expression of contractile genes is decreased in myometrium of WT or SRC-1/-2–deficient females bred to SRC-1/-2–deficient males. The contractile genes *Cx43*, *Oxtr*, and cyclooxygenase 2 (*Cox2*,

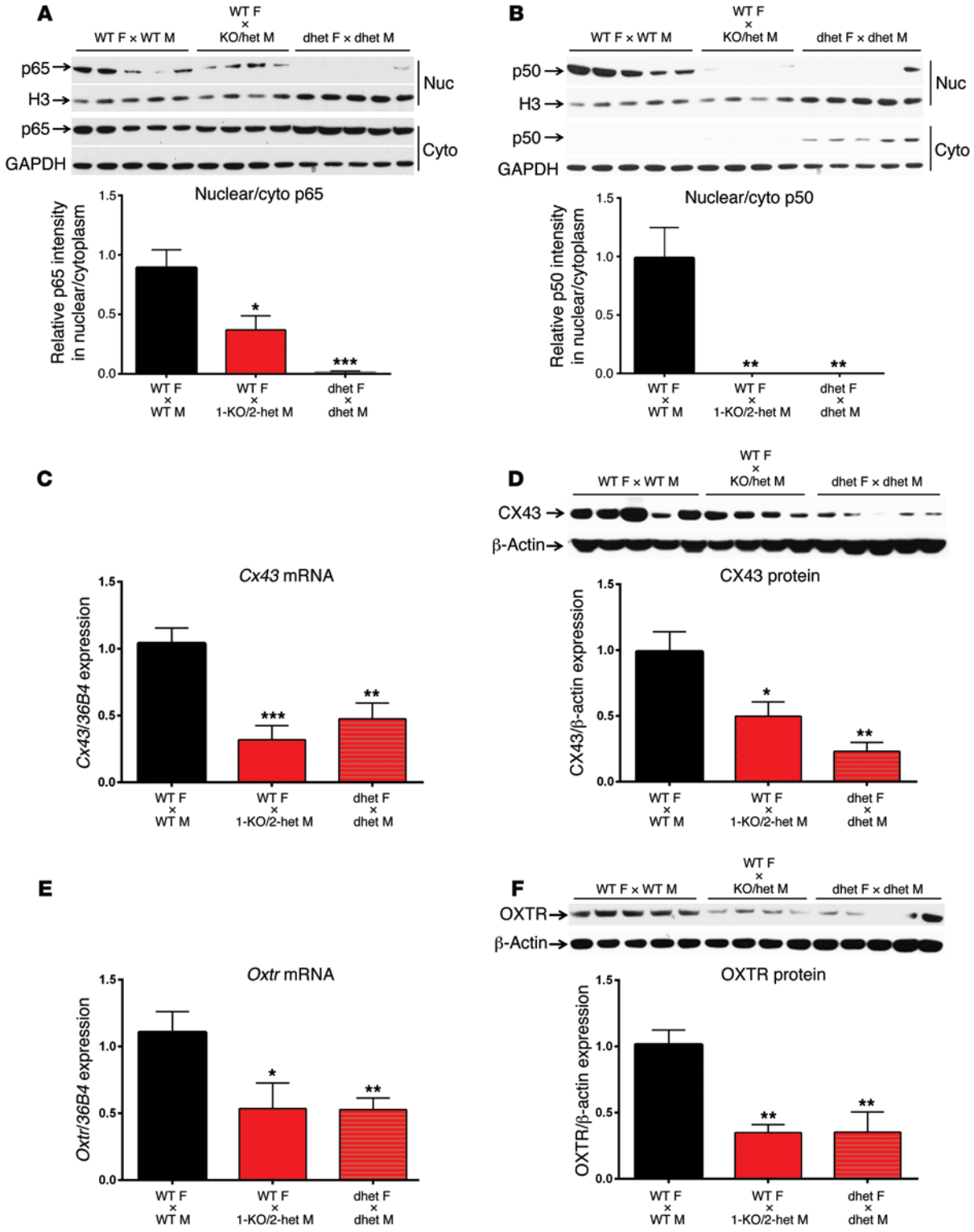

Figure 2. NF-κB activation and contraction-associated protein gene expression are decreased in 18.5 dpc pregnant myometrium of *SRC-1/-2* dhet females × *SRC-1/-2* dhet males and WT females × 1-KO/2-het males, compared with WT females × WT males. (**A** and **B**) Nuclear translocation of (**A**) NF-κB p65 and (**B**) p50 in myometrium. Representative immunoblots of p65 and p50 protein in nuclear (Nuc) or cytoplasmic (Cyto) fractions. The same immunoblots of histone H3 and GAPDH are shown for nuclear and cytoplasmic proteins, respectively, since p65 and p50 were probed on the same respective blots. Combined data from densitometric scans of nuclear immunoblots for p65 and p50 relative to cytoplasmic immunoblots, normalized to internal controls for WT females × WT males (n = 10), WT females × 1-KO/2-het males (n = 8), and dhet females × dhet males (n = 10). (**C**) *Cx43* mRNA and (**D**) protein levels for WT females × WT males (n = 5), WT females × 1-KO/2-het males (n = 4), and dhet females × dhet males (n = 5). The same immunoblot of β-actin (**D**) was used for the normalization of AKR1B3 (Figure 3B) and PGDH (Figure 3D), which were probed on same blot. (**E**) *Oxtr* mRNA and (**F**) protein in myometrium from WT females × WT males (n = 5), WT females × 1-KO/2-het males (n = 4), and dhet females × dhet males (n = 5). Densitometric scans were normalized to β-actin. Data are mean ± SEM. $^*P < 0.05$, $^{**}P < 0.01$, $^{***}P < 0.001$ (ANOVA).

also known as prostaglandin-endoperoxide synthase 2 [*Ptgs2*]), the critical enzyme in synthesis of contractile prostaglandins, which promote transformation of the myometrium from a quiescent state to a contractile unit, are known targets of NF-κB (34, 35). To determine the direct cause of delayed initiation of myometrial contraction in *SRC-1/-2*–deficient mice, the expression of these contractile genes in myometrium was analyzed. mRNA and protein levels of both CX43 and OXTR were significantly decreased in myometrium of *SRC-1/-2* dhet or WT females bred to 1-KO/2-het males compared with those in WT crosses (Figure 2, C–F), whereas no significant differences in *Cox2* mRNA or protein levels were detected among these groups of mice (Supplemental Figure 2, A and B). Interestingly, expression of the prostaglandin $F_2\alpha$-specific ($PGF_2\alpha$-specific) synthase, AKR1B3, was dramatically decreased, while that of the $PGF_2\alpha$-metabolizing enzyme, prostaglandin dehydrogenase (PGDH), was significantly increased in 18.5-dpc myometrium of *SRC-1/-2* dhet females bred to genetically matched males or WT females bred to 1-KO/2-het males (Figure 3, A–D). These changes were associated with a significant decrease in myometrial $PGF_2\alpha$ levels (Figure 3E).

Pregnant SRC-1/-2–deficient or WT females bred to SRC-1/-2–deficient males manifest delayed luteolysis, evidenced by increased ovarian StAR expression and serum P_4 levels at term. In a number of mammalian species, uterus-derived $PGF_2\alpha$ plays an important role in controlling luteolysis (36). In late gestation, activation of inflammatory response pathways leads to upregulation of uterine $PGF_2\alpha$, which then circulates to the ovary, in which it binds to $PGF_2\alpha$ receptors to initiate corpus luteum regression (36, 37). In rodents, P_4 production by the ovarian corpus luteum is maintained at high levels throughout pregnancy and diminishes near term, due to luteolysis. Increased P_4 production is maintained, in part, by steroidogenic acute regulatory protein (StAR), which facilitates translocation of cholesterol from the outer to the inner mitochondrial membrane, in which cholesterol is metabolized to pregnenolone by cholesterol side-chain cleavage (P450scc) (38, 39), the rate-determining step in steroidogenesis. StAR expression declines in the corpus luteum near term, with an associated fall in P_4 production (36). In this study, we found that circulating P_4 levels (Figure 3F) and ovarian StAR protein expression (Figure 3G) failed to decrease in *SRC-1/-2* dhet or WT females bred to *SRC-1/-2* dhet or 1-KO/2-het males, respectively. Using immunohistochemical analysis, we found prolonged StAR expression in the corpus luteum of the *SRC-1/-2* dhet females bred to *SRC-1/-2* dhet males (Figure 3H). This was clearly in contrast to WT mice, in which a pronounced decline in StAR expression occurred in late gestation (Figure 3H). Interestingly, *Star* mRNA expression was not significantly altered in ovaries of WT or *SRC-1/-2* dhet females bred to *SRC-1/-2* dhet or 1-KO/2-het males as compared with that of WT females bred to WT males near term (Supplemental Figure 3A). Similarly, $PGF_2\alpha$ was found to reduce StAR protein, but not mRNA, levels in rat luteal cells (40), suggesting posttranscriptional regulation. We also analyzed myometrial expression of the P_4-metabolizing enzyme 20α-hydroxysteroid dehydrogenase (20α-HSD), which increases in myometrium near term (41), but failed to observe significant changes in its protein levels with *SRC-1/-2* deficiency (Supplemental Figure 3C). Moreover, we correlated the degree of *SRC-1/-2* double deficiency (by the proportion of *SRC-1/-2* double-deficient fetuses in each litter) with circulating levels of maternal P_4 (as a measure of luteolysis) and found a strong positive correlation between P_4 levels and the degree of *SRC-1/-2* double deficiency (Supplemental Figure 3D). These collective findings suggest that fetal *SRC-1/SRC-2* deficiency inhibits a cascade of signals that promote increased $PGF_2\alpha$ production in the uterus and luteolysis at term. This results in maintenance of elevated circulating maternal P_4 in *SRC-1/-2*–deficient mice, which likely contributes to the delay in parturition.

LPCAT1 expression and synthesis of platelet-activating factor are reduced in lungs of SRC-1/-2–deficient fetuses. As mentioned, targeted deletion of the genes encoding SP-A and SP-D in mice also caused a significant delay in parturition (14.4 ± 4.3 hours) (15). However, WT females bred to 1-KO/2-het males manifested a much more striking delay in parturition (38.4 ± 1.0 hours) (Supplemental Figure 4), suggesting the potential roles of fetal signals other than SP-A and SP-D in the timing of labor. Indeed, the delay in parturition in the *SRC-1/-2* double-deficient mice may have been underestimated, since those pregnant mice that failed to deliver by 22.5 dpc were sacrificed. These differences in gestation length suggest the role(s) of fetal factors other than surfactant proteins in parturition timing.

Previously, it was observed that *SRC-1/SRC-2* dKO fetuses died at birth of apparent respiratory distress. The lungs of these fetuses manifested alveolar collapse (29), possibly due to impaired surfactant glycerophospholipid synthesis. To determine the enzyme(s) in the surfactant glycerophospholipid pathway that may be affected by the combined deficiency in SRC-1 and SRC-2, we analyzed expression of those enzymes catalyzing the key metabolic reactions. These included CTP:phosphocholine cytidylyltransferase α (CCTα), which catalyzes the condensation of CTP and phosphocholine to form CDP-choline; cholinephosphotransferase I (CHPT1), which catalyzes the reaction of CDP-choline and diacylglycerol to form phosphatidylcholine; and lysophosphatidylcholine acyltransferase-1 (LPCAT1), a key enzyme in surfactant phosphatidylcholine remodeling to form dipalmitoylphosphatidylcholine (DPPC), the major surface-active component of surfactant (42–44). Notably, neither CCTα nor CHPT1 manifested significant changes in expression in lungs of *SRC-1/-2* double-deficient fetuses compared with WT fetuses (Supplemental Figure 5, A and B). By contrast, *Lpcat1* mRNA and protein levels were markedly increased in WT fetal lungs at 18.5 dpc, compared with 15.5 dpc; however, this developmental increase failed to occur in lungs of *SRC-1/-2* double-deficient fetuses (Figure 4, A and B). This developmental induction of LPCAT1 in WT mice was consistent with a previous report indicating that LPCAT1 was developmentally regulated in the fetal lung and expressed specifically in type II cells (43). Intriguingly, we observed that expression of *Lpcat1* mRNA and protein was significantly decreased in lungs of *SRC-1/-2* double-deficient fetuses compared with that of WT fetuses (Figure 4, C and D). By using liquid chromatography mass spectrometry (LC-MS), we observed that DPPC concentrations were dramatically decreased in AF surrounding *SRC-1/-2* dhet and *SRC-1/-2* dKO fetuses at 18.5 dpc (3.54 ± 1.68 ng/μl and 2.70 ± 0.67 ng/μl, respectively, $P < 0.0001$), compared with WT fetuses (9.05 ± 1.80 ng/μl), while DPPC levels in AF surrounding

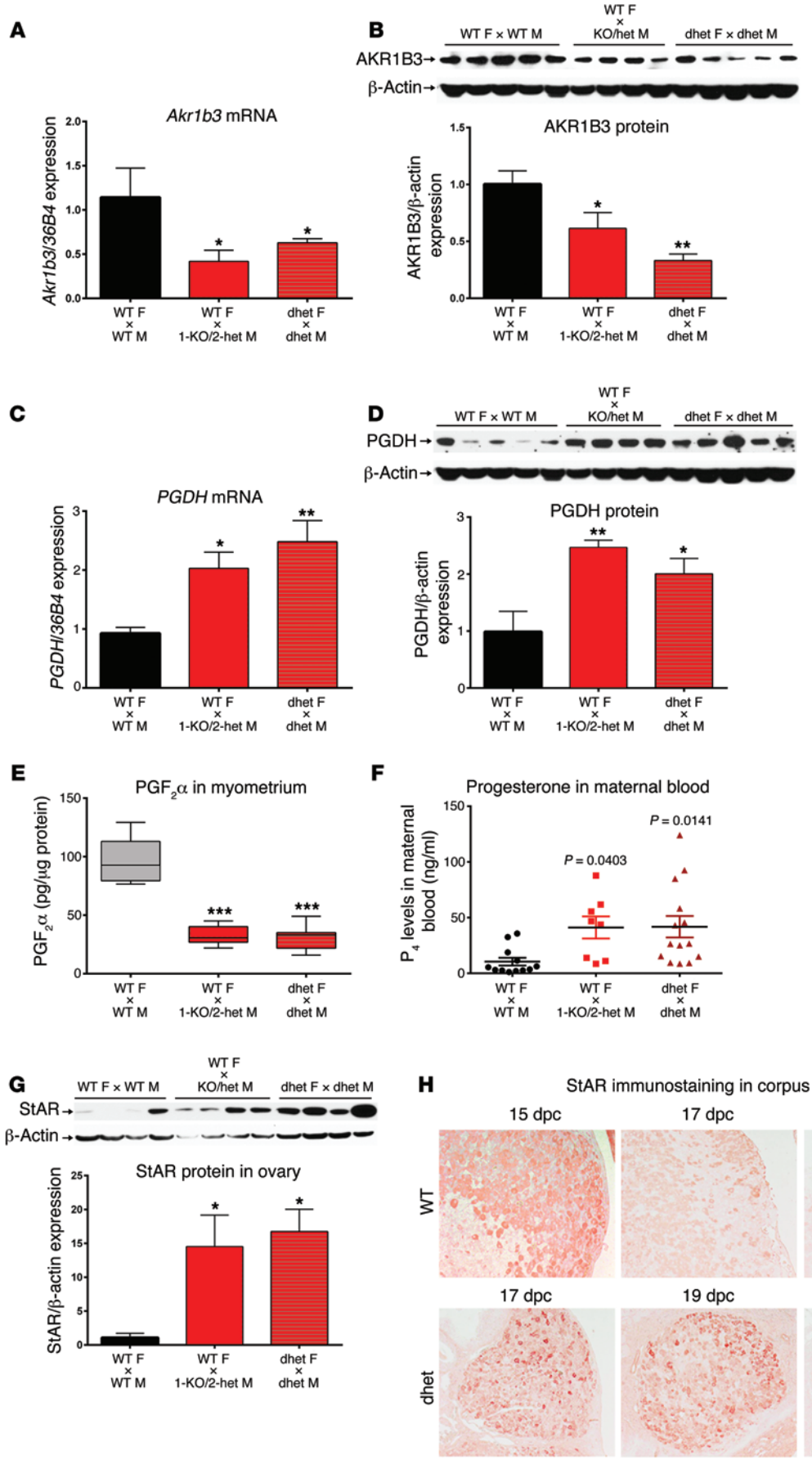

Figure 3. *SRC-1/-2* dhet or WT females bred to dhet or 1-KO/2-het males, respectively, manifest decreased myometrial $PGF_2\alpha$ synthesis and delayed ovarian luteolysis. (**A**) *Akr1b3* mRNA and (**B**) protein in myometrium from WT females × WT males (n = 5), WT females × 1-KO/2-het males (n = 4), and dhet females × dhet males (n = 5). Immunoblots and densitometric scans normalized to β-actin are shown. (**C**) *PGDH* mRNA and (**D**) protein in myometrium of WT females × WT males (n = 5), WT females × 1-KO/2-het males (n = 4), and dhet females × dhet males (n = 5). Immunoblots and densitometric scans normalized to β-actin are shown. (**E**) $PGF_2\alpha$ levels in myometrial homogenates normalized to protein for WT females × WT males (n = 12), WT females × 1-KO/2-het males (n = 8) and dhet females × dhet males (n = 15). In the box-and-whisker plot, horizontal bars indicate the medians, boxes indicate 25th to 75th percentiles, and whiskers indicate 10th and 90th percentiles. (**F**) Maternal serum P_4, measured by ELISA for WT females × WT males (n = 12), WT females × 1-KO/2-het males (n = 8), and dhet females × dhet males (n = 14). (**G**) StAR protein in ovaries. Representative immunoblot of StAR, and densitometric scans of StAR immunoblots normalized to β-actin (n = 8 per group). (**H**) At 17 and 19 dpc, StAR immunostaining in corpus luteum of *SRC-1/-2* dhet females × *SRC-1/-2* dhet males (dhet) was more intense than that of WT. Three independent experiments conducted. Original magnification, ×200. Data are mean ± SEM. $^*P < 0.05$, $^{**}P < 0.01$, $^{***}P < 0.001$ (ANOVA).

SRC-1$^{-/-}$ fetuses (8.87 ± 1.81 ng/μl) were comparable to those of WT fetuses (Supplemental Figure 5C).

LPCAT1 also catalyzes the synthesis of platelet-activating factor (PAF) from lyso-PAF and acetyl-CoA (45). PAF, an inflammatory phospholipid, was previously reported to increase in AF near term and play a role in the initiation of term and preterm labor (46–50). In the present study, we similarly observed that PAF levels in fetal lungs and AF were significantly increased at 18.5 dpc compared with earlier time points in fetuses from WT crosses (Figure 4, E and F) but failed to increase in lungs and AF of *SRC-1/-2* dhet or *SRC-1/-2* dKO fetuses at 18.5 dpc (Figure 4, G and H). By contrast, the related acyltransferase enzyme, LPCAT2, believed to catalyze PAF synthesis in response to proinflammatory stimuli, as well as the PAF-degrading enzyme, PAF acetylhydrolase (PAFAH), were unaffected by *SRC-1/-2* double deficiency in fetal lung (Supplemental Figure 5, D and E). Besides LPCAT1, expression of several enzymes associated with the de novo pathway of PAF biosynthesis (51), including ABCD2 (also known as ALDRP), a peroxisomal ATP-binding cassette transporter, which is suggested to be involved in the transport of very-long-chain acyl-CoA (52), also was analyzed; however, no differences were observed in the lungs of *SRC-1/-2* dKO or dhet fetuses compared with WT fetuses (Supplemental Figure 5F).

These findings provide compelling evidence that the fetus signals the mother when its lungs develop the capacity to produce sufficient surfactant to sustain air breathing and that SRC-1 and SRC-2 serve a crucial and specific role through transcriptional regulation of *SP-A* and *LPCAT1*.

SRC-1 and SRC-2 enhance Lpcat1 promoter transactivation by glucocorticoids in a GRE-dependent manner. As mentioned above, we previously observed that SRC-1 and SRC-2 serve important roles in transcriptional upregulation of *SP-A* gene expression in fetal lung type II cells (20, 21). Although the *Lpcat1* gene was cloned from mouse fetal lung 9 years ago (43, 44) and found to be highly expressed in lung type II cells and regulated by glucocorticoids (43), the mechanisms underlying its transcriptional regulation are largely undefined. Using the MatInspector program, we identified 5 putative glucocorticoid response elements (GREs), between –1,000 and –2,000 bp upstream of the mouse *Lpcat1* transcription start site, as well as a putative P_4 response element and androgen response element, between –1,000 bp and the transcription start site (Figure 5A). To functionally define the glucocorticoid-responsive region(s), different lengths of *Lpcat1* 5′-flanking sequence (2.0 kb, 1.0 kb, 0.6 kb, 0.4 kb) were subcloned into the pGL4.12 luciferase vector and cotransfected into lung adenocarcinoma A549 cells, together with Renilla luciferase plasmid. Cells expressing these *Lpcat1* promoter constructs, as well as empty vector, were treated with or without dexamethasone (Dex, 10^{-7} M) for 24 hours, and luciferase activity was analyzed using a Dual Luciferase Reporter Assay System. Luciferase activities of all *Lpcat1* promoter constructs were comparably increased above empty vector (Supplemental Figure 6); however, only the *Lpcat1*$_{-2000}$*-Luc* plasmid containing all 4 putative GREs was upregulated by Dex treatment (Figure 5A). Moreover, when A549 cells were transfected with *Lpcat1*$_{-2000}$*:Luc* reporters, with or without mutation in GRE4 and GRE5 and cultured with or without Dex (10^{-7} M) for 24 hours, mutagenesis of GRE4 and GRE5 prevented Dex induction of *Lpcat1* promoter activity (Figure 5B). The roles of endogenous SRC-1 and SRC-2 in glucocorticoid induction of *Lpcat1* were suggested by the finding that siRNA-mediated knockdown of endogenous SRC-1, SRC-2, or both SRC-1 and SRC-2 blocked the inductive effect of Dex on *Lpcat1* promoter activity (Figure 5B). This was analyzed by transfecting A549 cells with preannealed siRNA duplexes for SRC-1 and SRC-2, followed by transfection with *Lpcat1*$_{-2000}$*:Luc* construct and Renilla luciferase, treatment with or without Dex for 24 hours, and assay of luciferase.

To assess binding of endogenous glucocorticoid receptor (GR), SRC-1, and SRC-2 to the putative GREs, ChIP–quantitative PCR (ChIP-qPCR) was carried out in lung tissues from WT and *SRC-1/-2* dKO fetal mice at 18.5 dpc using primers flanking each of these sites. As can be seen, endogenous GR, SRC-1, and SRC-2 bound specifically to GRE4 and GRE5 within the *Lpcat1* promoter in fetal lung tissues of WT mice but not *SRC-1/-2*–deficient mice (Figure 5, C–E).

To determine whether the human *LPCAT1* gene also is regulated by glucocorticoids and assess the roles of SRC-1 and SRC-2 in this regulation, we used primary cultures of HFL type II cells infected with lentivirus containing shRNA targeting SRC-1 and/or SRC-2 and cultured them with or without Dex, in the absence or presence of the GR/PR antagonist, RU486. Dex significantly increased the mRNA and protein expression of LPCAT1 after 24 hours of treatment, and this was completely blocked by RU486 (Figure 5, F and G). In contrast, expression of LPCAT2 was not affected by Dex or by RU486 treatment (Supplemental Figure 7A). Efficient knockdown of either SRC-1 or SRC-2 (each was decreased by more than 95%, Supplemental Figure 7B) partially blocked the inductive effects of Dex on LPCAT1 expression; knockdown of both SRC-1 and SRC-2 had a more pronounced effect (Figure 5, H and I), again, suggesting possible compensatory upregulation of SRC-1 and SRC-2.

i.a. injection of SP-A and PAF at 17.5 dpc rescues the delayed-labor phenotype and downstream pathways in SRC-1/-2–deficient mice. We previously reported that i.a. injection of purified SP-A at 15.5 dpc caused preterm delivery of fetuses within 6 to 24 hours (6). In light of our findings that SP-A and PAF levels were decreased in AF surrounding *SRC-1/-2*–deficient fetuses, we evaluated whether administration of exogenous SP-A or PAF could rescue the delayed-labor phenotype of *SRC-1/-2*–deficient mice. SP-A (3 μg per sac), containing <3 fg LPS per microgram of SP-A (after polymyxin B treatment) (6), or methylcarbamyl PAF-C-16 (0.25 ng per sac) was injected i.a. into *SRC-1/-2*–deficient mice at 17.5 dpc; this corresponds to the approximate time that SP-A (6) and PAF (Figure 4F) naturally increase in AF. The amounts of SP-A and PAF injected were calculated to result in AF concentrations comparable to those normally found at term (~15 μg/ml [ref. 6] and 1.25 ng/ml [Figure 4F], respectively). A parallel group of *SRC-1/-2*–deficient mice were injected i.a. with an equivalent volume of sterile PBS, the solvent for both SP-A and methylcarbamyl PAF-C-16. Four of ten *SRC-1/-2*–deficient mice injected with SP-A delivered premature fetuses surrounded by intact amniotic membranes at 18.5 to 19.0 dpc, and the remaining 6 mice delivered at term on 19.5 dpc. Similarly, 3 of 10 mice injected with PAF delivered at 18.5 to 19 dpc, and the remaining 7 mice delivered at term on 19.5 dpc (Figure 6A). Only the left uterine horn was injected, while the right horn was left uninjected as an internal control. As reported

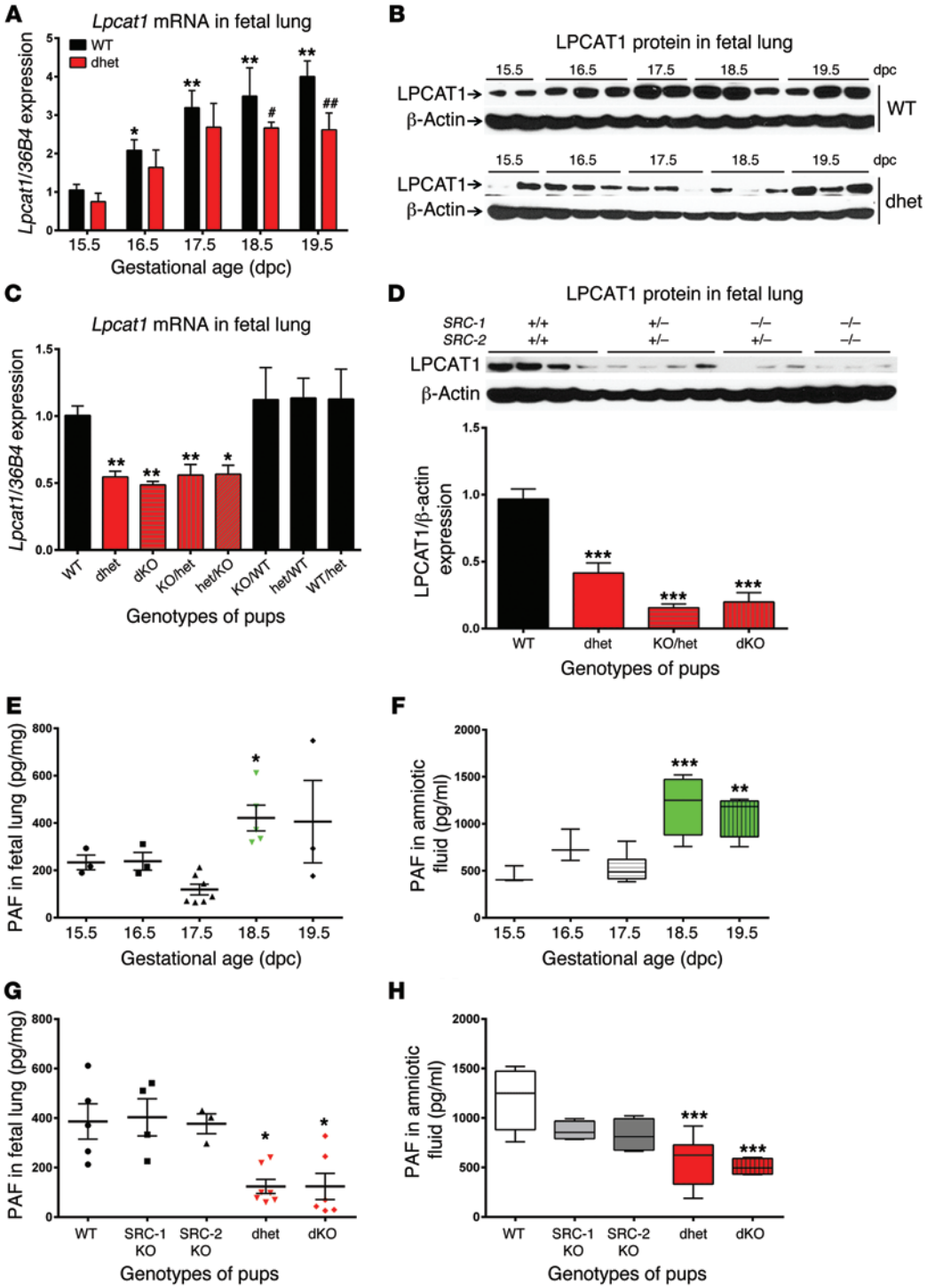

Figure 4. LPCAT1 expression and PAF synthesis and secretion are reduced in lungs of *SRC-1/-2* double-deficient fetuses. (**A**) *Lpcat1* mRNA in lungs of WT and *SRC-1/-2* dhet (dhet) fetuses from 15.5 dpc to term (n = 5 mice per time point). (**B**) Representative immunoblot of LPCAT1 protein in lungs of WT or *SRC-1/-2* dhet fetuses from 15.5 dpc to term (n = 2–3 per time point). (**C**) *Lpcat1* mRNA in lungs of 18.5 dpc WT (n = 3), dhet (n = 14), dKO (n = 3), KO/het (n = 6), het/KO (n = 6), KO/WT (n = 3), het/WT (n = 13), and WT/het (n = 4) fetuses. (**D**) LPCAT1 protein in fetal lungs at 18.5 dpc. Representative immunoblot according to genotype, and densitometric scans of immunoblots of LPCAT1 normalized to β-actin for WT (n = 7), dhet (n = 8), KO/het (n = 8), and dKO (n = 4) fetuses are shown. (**E**) PAF in WT fetal lungs at 15.5 (n = 3), 16.5 (n = 3), 17.5 (n = 7), 18.5 (n = 5), and 19.5 (n = 3) dpc. (**F**) PAF in AF surrounding WT fetuses at 15.5 (n = 3), 16.5 (n = 3), 17.5 (n = 7), 18.5 (n = 6), and 19.5 (n = 4) dpc. (**G**) PAF in 18.5 dpc fetal lungs of WT (n = 5), *SRC-1* KO (n = 4), *SRC-2* KO (n = 3), dhet (n = 7), and dKO (n = 6). (**H**) PAF in AF surrounding 18.5 dpc WT (n = 6), *SRC-1* KO (n = 4), *SRC-2* KO (n = 4), dhet (n = 6), and dKO (n = 5) fetuses. (**F** and **H**) In the box-and-whisker plots, horizontal bars indicate the medians, boxes indicate 25th to 75th percentiles, and whiskers indicate 10th and 90th percentiles. Data are mean ± SEM. $^{*}P < 0.05$, $^{**}P < 0.01$, $^{***}P < 0.001$; $^{\#}P < 0.05$, $^{\#\#}P < 0.01$ compared with WT at same dpc (ANOVA).

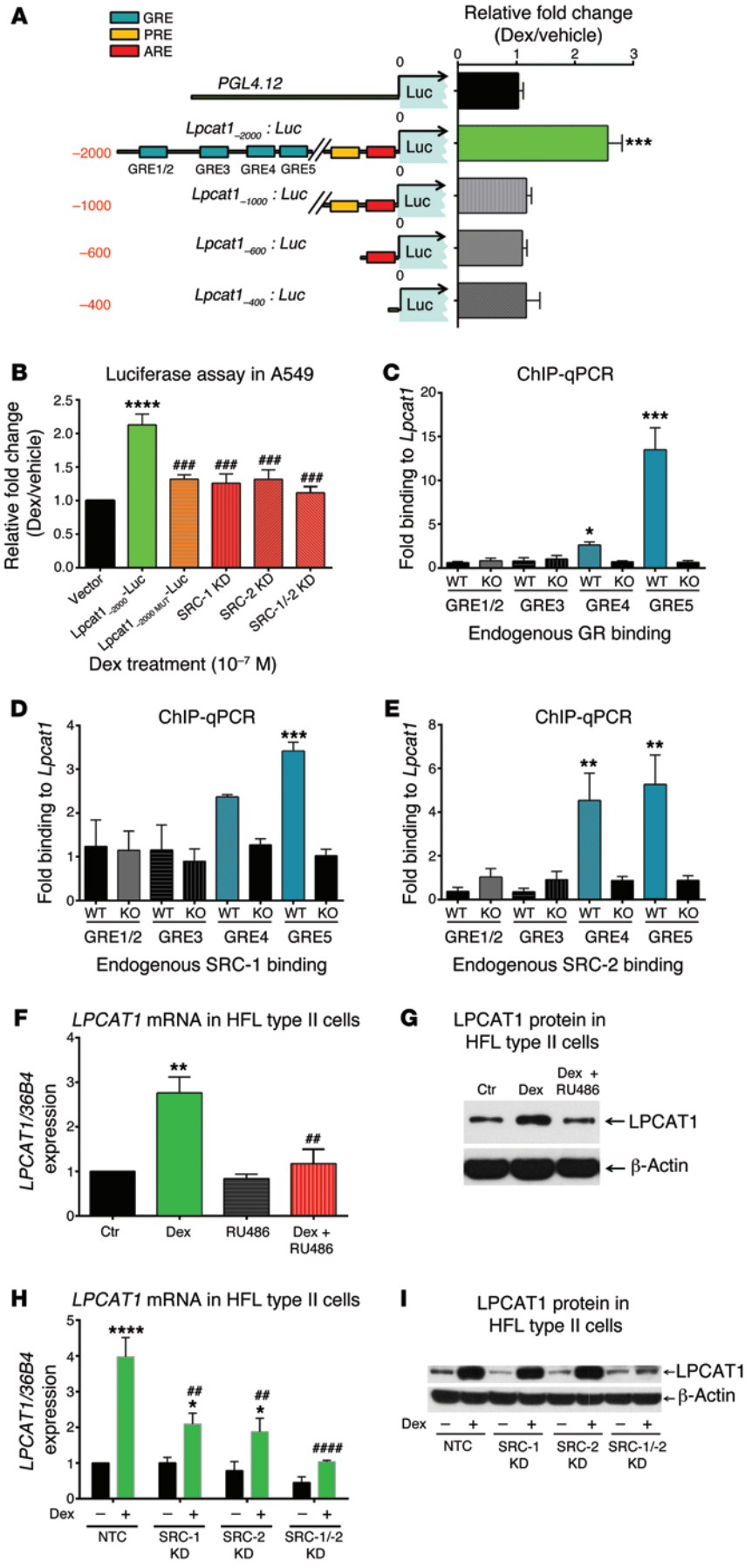

Figure 5. SRC-1 and SRC-2 enhance *Lpcat1* promoter transactivation and expression by glucocorticoids in a *GRE*-dependent manner. (**A**) *Lpcat1*:luciferase reporter constructs containing various amounts of 5′-flanking sequence of the mouse *Lpcat1* gene; putative GREs, androgen response elements (ARE), and P_4 response element (PREs) are indicated. A549 cells cotransfected with these constructs and Renilla luciferase were treated with or without Dex (10^{-7} M) for 24 hours; luciferase assays were performed (n = 4 for each construct). (**B**) Effects of mutation of GRE4 and GRE5 (*Lpcat1*$_{-2000MUT}$*-Luc*)and knockdown (KD) of SRC-1, SRC-2, or SRC-1 and SRC-2 on Dex-induced *Lpcat1* promoter activity (n = 4, each construct). Data are mean ± SEM. (**C**–**E**) ChIP-qPCR of WT or *SRC-1/-2* dKO (KO) fetal lung tissues using antibodies to (**C**) GR, (**D**) SRC-1, or (**E**) SRC-2 and specific primers for GRE1/2, GRE3, GRE4, or GRE5 within the *Lpcat1* promoter (n = 4). (**F**) *LPCAT1* mRNA levels in HFL type II cells treated with Dex with or without RU486 (n = 5). (**G**) Representative immunoblot of LPCAT1 protein in HFL type II cells treated with Dex with or without RU486. Five independent experiments were conducted. (**H**) *LPCAT1* mRNA in HFL type II cells infected with recombinant lentiviruses expressing SRC-1 and/or SRC-2 shRNA and cultured with or without Dex (10^{-7} M) (n = 4). NTC, silencer negative control siRNA. (**I**) Representative immunoblot of LPCAT1 protein in HFL type II cells infected with recombinant lentiviruses expressing SRC-1 or SRC-2 shRNA, cultured with or without Dex (n = 4). Data are mean ± SEM. $^{*}P < 0.05$, $^{**}P < 0.01$, $^{***}P < 0.001$, $^{****}P < 0.0001$; $^{\#\#}P < 0.01$ compared with Dex treatment alone; $^{\#\#\#}P < 0.001$ compared with cells expressing WT *Lpcat1*$_{-2000}$*-Luc* and *Silencer* negative control siRNA (ANOVA).

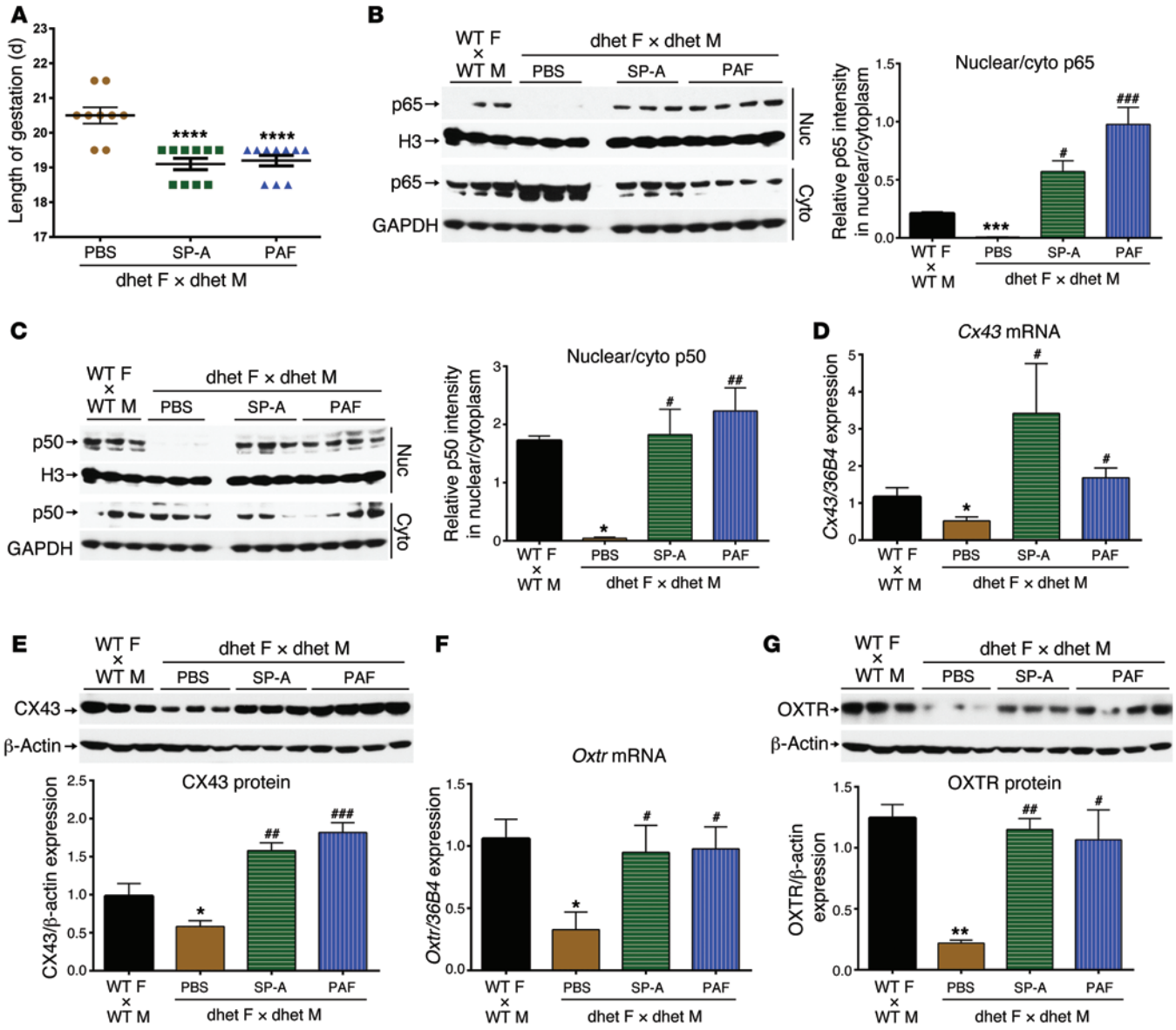

Figure 6. Delayed parturition and decreased NF-κB activation and expression of *Cx43* and *Oxtr* in *SRC-1/-2* dhet females bred to *SRC-1/-2* dhet males are rescued by i.a. injection of SP-A or PAF at 17.5 dpc. (**A**) Gestation length of *SRC-1/-2* dhet females × *SRC-1/-2* dhet males injected i.a. at 17.5 dpc with PBS (n = 9), SP-A (n = 10), or PAF (n = 10). (**B** and **C**) Nuclear translocation of NF-κB subunits p65 and p50 in 18.5 dpc myometrial tissues of WT females × WT males (uninjected, n = 3) or *SRC-1/-2* dhet females × *SRC-1/-2* dhet males injected i.a. with PBS (n = 3), SP-A (n = 3), or PAF (n = 4) at 17.5 dpc. The same immunoblots of loading controls, histone H3, and GAPDH are shown for nuclear and cytoplasmic proteins, respectively, since p65 and p50 were probed on the same respective blots. (**D**) *Cx43* mRNA levels (n = 6 per group) and (**E**) protein levels (n = 3 for WT, PBS, and SP-A; n = 4 for PAF) in myometrium. The same immunoblot of β-actin was used for normalization of OXTR (**G**), which was probed on the same blot. (**F**) *Oxtr* mRNA (n = 6 per group) and (**G**) protein (n = 3 for WT, PBS, and SP-A; n = 4 for PAF) in myometrium. Data are the mean ± SEM. $^{*}P < 0.05$, $^{**}P < 0.01$, $^{***}P < 0.001$, $^{****}P < 0.0001$ compared with WT; $^{\#}P < 0.05$, $^{\#\#}P < 0.01$, $^{\#\#\#}P < 0.001$ compared with PBS injection (ANOVA).

previously for SP-A (6) and as observed in the present study for SP-A or PAF treatment, only the fetuses in the injected horn delivered prematurely — or on time in the case of *SRC-1/SRC-2* double deficiency. Only 2 of 9 *SRC-1/-2*–deficient mice injected i.a. with sterile PBS manifested normal term labor (19.5 dpc), whereas the remaining 7 delivered 1 to 2 days late (Figure 6A).

Furthermore, we found that SP-A or PAF injection significantly reversed the inhibitory effects of *SRC-1/-2* deficiency on myometrial NF-κB activation (Figure 6, B and C), contractile gene expression (Figure 6, D–G), and the expression of $PGF_2\alpha$ synthase, AKR1B3 (Figure 7, A and B). Meanwhile, the increased expression of the $PGF_2\alpha$-metabolizing enzyme, PGDH, in myometrium of *SRC-1/-2* dhet females bred to *SRC-1/-2* dhet males also was prevented by SP-A or PAF injection (Figure 7, C and D); this resulted in an upregulation of $PGF_2\alpha$ levels in myometrium (Figure 7E). Consequently, i.a. SP-A or PAF injection caused a decrease in ovarian StAR protein (Figure 7F) and circulating P_4 (Figure 7G) to levels comparable to those of WT mice. By contrast, PBS injection had no effect on any of these parameters. Again, *Star* mRNA expression in ovaries of *SRC-1/-2* dhet females bred to *SRC-1/-2* dhet males was

not significantly altered by SP-A or PAF injection (Supplemental Figure 3B). Based on these findings and the correlation of gestation length with the proportion of *SRC-1/-2*–deficient pups in the litter (Figure 1C), we postulate that secretion of both SP-A and PAF by the maturing fetal lung near term provides a key stimulus for activation of contractile genes in the maternal uterus. Supplementation with either factor was sufficient to rescue the delay in labor in *SRC-1/-2*–deficient mice.

Discussion

Mice in which *SRC-1* and *SRC-2* have both been knocked out die at birth of respiratory distress (29). To investigate the mechanisms whereby deficiency of SRC-1 and SRC-2 cause decreased production of pulmonary surfactant components, we crossed *SRC-1/-2* dhet mice. Surprisingly, the mice exhibited a highly pronounced delay in parturition. Noteworthily, WT females bred to *SRC-1/-2* double-deficient males (1-KO/2-het) manifested an equivalently severe delay in labor. Notably, the proportion of "double-deficient" fetuses produced by crossing WT females with 1-KO/2-het males was estimated to be similar to that of the *SRC-1/-2* dhet crosses (50% vs. 56.25%, respectively), even though there are no *SRC-1/-2* dKO fetuses produced in the former. Moreover, SP-A and PAF levels were significantly and comparably decreased in lungs and AF samples from all double-deficient (*SRC-1/-2* dhet, 1-het/2-KO, 1-KO/2-het, and *SRC-1/-2* dKO) fetuses compared with those in single-deficient (*SRC-1*$^{-/-}$ and *SRC-2*$^{-/-}$) or WT pups. These findings strongly suggest that the delay in parturition timing was caused by a deficiency in fetus-derived factors in lungs of the *SRC-1 SRC-2* double-deficient pups. The role of the fetus was further supported by the positive correlation found between the proportion of *SRC-1/-2*–deficient pups in the litters and gestational length.

Although a number of reproduction-related phenotypes have been elucidated in *SRC-1* and *SRC-2* KO mice (24), the combined and cooperative functions of SRC-1 and SRC-2 in pregnancy and parturition have not been explored. The present finding that double deficiency in SRC-1 and SRC-2 is required for manifestation of the delayed parturition phenotype suggests the presence of compensatory mechanisms and cooperative physiological functions between SRC-1 and SRC-2 in the regulation of gestation length. This is consistent with a previous study showing that endogenous SRC-2 overexpression in certain tissues of *SRC-1*–null mutants compensated partially for the loss of SRC-1 (26) as well as our current findings that KO of one coregulator in fetal lung caused marked compensatory upregulation of the other. Moreover, we observed that efficient knockdown of both SRC-1 and SRC-2 had a more pronounced effect to reduce Dex-induced LPCAT1 expression than knockdown of either SRC-1 or SRC-2 alone.

Both term and preterm labor in humans and rodents are mediated by an inflammatory response, associated with elevated levels of proinflammatory cytokines in AF and increased leukocyte migration into the myometrium (11). Increasing evidence suggests that the developing fetus may provide physical and hormonal signals that activate inflammatory transcription factors in myometrium and contribute to the induction of spontaneous labor at term. Previously, we suggested that the major surfactant protein, SP-A, a developmentally regulated C-type lectin involved in innate immunity within the lung alveolus, plays an important role in initiating labor at term by activating fetal macrophages and promoting their migration to the maternal uterus (6). Moreover, mice that were globally deficient in the genes encoding SP-A and the related C-type lectin, SP-D, manifested a significant delay in parturition, accompanied by decreased AF macrophage activation and a marked reduction in myometrial proinflammatory and contraction-associated gene expression (15).

As mentioned, *SP-A* transcription in fetal lung type II cells was previously found to be enhanced by SRC-1 (21) and SRC-2 (20). Accordingly, in the present study, *SP-A* mRNA and protein expression and secretion into AF were observed to be significantly reduced in lungs of fetuses deficient in both SRC-1 and SRC-2. The marked delay in parturition also was associated with decreased myometrial NF-κB activation and a lack of induction of the contraction-associated genes *Cx43*, *Oxtr*, and *Akr1b3* near term. Consequently, ovarian StAR protein levels failed to decline near term and circulating P_4 levels remained elevated, due to a block in luteolysis.

While reduced SP-A expression in lungs of *SRC-1/-2*–deficient fetuses likely contributed to the delay in parturition, the effect of *SRC-1/-2* deficiency on parturition timing (~38-hour delay) was considerably greater than that observed with *SP-A* or *SP-A/SP-D* dKO mice (~12-hour delay) (15). These pronounced differences suggested that other fetal signals contribute to the timing of labor. Previous studies by Johnston and colleagues suggested that PAF, produced in increasing amounts by the developing fetal lung and secreted into AF, may play a role in the initiation of term and preterm labor (46–50). Importantly, we observed that levels of PAF in fetal lungs and AF of *SRC-1/-2* double deficient mice failed to increase and were significantly reduced as compared with those of WT or *SRC-1* or *SRC-2* single-deficient fetuses near term. PAF has been observed to enhance cytokine production and migration of polymorphonuclear leukocytes (PMNs) into the cervix at the time of parturition (53–55). Studies with PAF receptor KO mice suggested that PAF is a direct mediator of PMN activation (56). Moreover, unlike other inflammatory mediators (e.g., cytokines or LPS), PAF is a direct uterotonic agent (57–60). PAF also has been implicated in preterm parturition because its levels are increased in the AF of women in preterm labor (47, 61). Thus, PAF and SP-A produced by fetal lung type II cells may cooperatively act to enhance migration of macrophages and other leukocytes to the myometrium near term. Notably, we observed that i.a. injection of PAF or SP-A at 17.5 dpc corrected the parturition delay in *SRC-1/-2*–deficient mice. Moreover, rescue of the parturition delay in *SRC-1/-2* dhet females bred to *SRC-1/-2* dhet males by SP-A or PAF i.a. injection at 17.5 dpc restored NF-κB activation, CX43 and OXTR expression in the maternal myometrium, StAR expression in the ovary, and circulating P_4 levels to WT values at 18.5 dpc.

In studies to define the underlying mechanisms for PAF upregulation in fetal lung near term and the effects of *SRC-1/-2* deficiency, we discovered that LPCAT1, a key enzyme in the acylation of the *sn-2* position of both DPPC and PAF (42–44), was significantly decreased in lungs of *SRC-1/-2* dKO fetuses compared with that in WT fetuses. LPCAT1 was previously reported to be developmentally upregulated in mouse fetal lung, selectively expressed in type II cells, and increased by glucocorticoids (43). In studies using HFL type II cells, we observed that Dex induced LPCAT1 expression in a GR/SRC-1/-2–dependent manner. Glucocorticoid upreg-

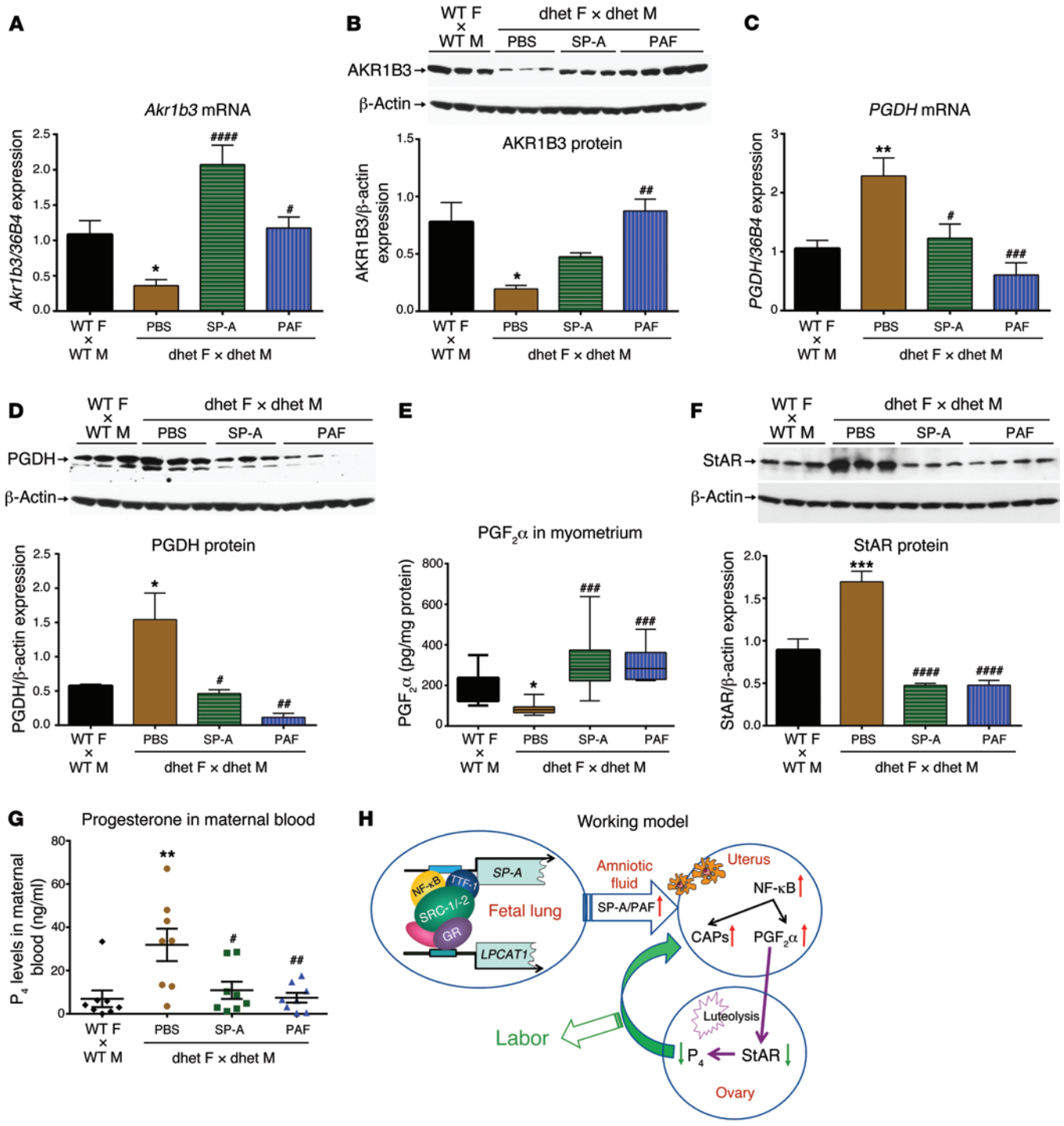

Figure 7. Rescue of parturition delay in *SRC-1/SRC-2* dhet females bred to *SRC-1/-2* dhet males is associated with increased myometrial $PGF_2\alpha$ synthesis and decreased ovarian P_4 production. (**A**) *Akr1b3* mRNA (n = 6 per group) and (**B**) protein (n = 3 for WT, PBS, and SP-A; n = 4 for PAF) in myometrium. The same immunoblot of β-actin was used for normalization of PGDH (**D**), which was probed on the same blot. (**C**) *PGDH* mRNA (n = 6 per group) and (**D**) protein (n = 3 for WT, PBS, and SP-A; n = 4 for PAF) in myometrium. (**E**) $PGF_2\alpha$ levels in myometrial homogenates for WT or *SRC-1/-2* mice injected i.a. with PBS, SP-A, or PAF (n = 8 per group). In the box-and-whisker plot, horizontal bars indicate the medians, boxes indicate 25th to 75th percentiles, and whiskers indicate 10th and 90th percentiles. (**F**) StAR protein in ovaries of WT (n = 3) or *SRC-1/-2* dhet females × *SRC-1/-2* dhet males injected i.a. with PBS (n = 3), SP-A (n = 3), or PAF (n = 4). (**G**) Maternal serum P_4 levels, measured by ELISA, of 18.5 dpc WT females × WT males or *SRC-1/-2* dhet females × *SRC-1/-2* dhet males injected i.a. with PBS, SP-A, or PAF (n = 8 per group). (**H**) Proposed cooperative roles of SRC-1 and SRC-2 in the initiation of labor through regulation of *SP-A* and *Lpcat1* gene expression. Data are the mean ± SEM. $^{*}P < 0.05$, $^{**}P < 0.01$, $^{***}P < 0.001$, compared with WT; $^{\#}P < 0.05$, $^{\#\#}P < 0.01$, $^{\#\#\#}P < 0.001$, $^{\#\#\#\#}P < 0.0001$ compared with PBS injection (ANOVA).

ulation of *LPCAT1* promoter activity was mediated by two consensus GRE repeats that bound GR, SRC-1, and SRC-2 in a cooperative manner. Previous findings that *SRC-1* and *SRC-2* KO mice manifested hyposensitivity to glucocorticoids (62) further suggest that compromised action of glucocorticoids in *SRC-1/-2*–deficient mice may contribute to decreased *LPCAT1* expression. Fetal plasma glucocorticoids increase exponentially during late gestation (14) and are thought to serve a role in maturation of the fetal lungs (63–68). Neonatal mice in which *SRC-1* and *SRC-2* were both knocked out were reported to have diffuse lung atelectasis and died at birth of apparent respiratory distress (29). Importantly, we observed that the decreased expression of LPCAT1 in lungs of *SRC-1/-2*–deficient fetuses was associated with profoundly reduced secretion of DPPC into AF. Since DPPC is the most surface-active component of pulmonary surfactant, this decline in DPPC production is likely responsible for the alveolar collapse observed in *SRC-1/-2* dKO mice. The importance of LPCAT1 in fetal lung is supported by the finding that mice homozygous for a hypomorphic allele of *Lpcat1* manifested varying perinatal mortality from respiratory distress, associated with a deficiency in surfactant DPPC (42). In light of the pleiotrophic effects of SRC-1 and SRC-2, it is likely that the actions of other transcription factors are compromised in lungs of the double-deficient mice, contributing to the impaired production of surfactant components. While our study revealed important roles of SP-A and PAF in signaling the initiation of labor, it is likely that SRC-1 and SRC-2 have additional fetal target genes besides *SP-A* and *LPCAT1* that might contribute to the parturition delay. Genome-wide RNA-seq analysis of lung tissues of *SRC-1/-2* dKO and WT fetuses will be used to identify other possible target genes and provide a more comprehensive view of the coordinated roles of SRC-1 and SRC-2 in the timing of labor.

In conclusion, our findings provide compelling evidence that the fetus initiates parturition by signaling the mother when its lungs develop the capacity to produce sufficient surfactant lipoprotein to sustain air breathing. This likely occurs through the production of two fetal lung-derived factors — SP-A and PAF (Figure 7H). Both of these factors have the capacity to activate immune cells, resulting in an enhanced inflammatory response within the maternal uterus, as well as a decline in PR function, which collectively result in increased expression of myometrial contractile genes and the initiation of labor. The coactivators SRC-1 and SRC-2 serve crucial roles in this process through transcriptional regulation of genes encoding SP-A and LPCAT1, a key regulatory enzyme in the synthesis of DPPC, which is the major surface-active component of surfactant, and PAF, a proinflammatory glycerophospholipid (Figure 7H).

Methods

Timing of labor in SRC-1/-2–deficient and WT mice. To examine the effects of deficiencies in SRC-1 and/or SRC-2 on the timing of labor, SRC-1 homozygous KO (*SRC-1*$^{-/-}$), SRC-2 heterozygous (*SRC-2*$^{+/-}$), and *SRC-1/-2* dhet females (B6 background) were bred to genetically matched males. To determine whether phenotypic effects were caused by deficiencies in the fetuses, WT females also were bred to 1-KO/2-het males. WT B6 females were bred to WT males as controls. Breeding pairs were placed together at 1800 hours and separated the following morning at 0600 hours. Pregnancy was suggested by the presence of a vaginal plug; gestational age was designated at that time as 0.5 dpc. The time to labor was documented upon delivery of the first pup or by the presence of a litter. All mice were housed under pathogen-free conditions, maintained on a 12-hour-dark/12-hour-light cycle, and allowed free access to a standard pellet chow.

Collection of AF, myometrium, ovaries, sera, and fetal lungs at 15.5 to 18.5 dpc. Parturition timing was assessed in first pregnancies, while fluids and tissues were analyzed in second pregnancies. AF, myometrium, ovaries, sera, and fetal lungs were collected from timed-pregnant mice at approximately 1000 hours at 15.5, 16.5, 17.5, and 18.5 dpc. Uteri were exposed and AF from individual amniotic sacs was carefully aspirated, avoiding maternal blood contamination, using a 20-gauge needle and a 1.0-ml syringe. Maternal myometrium was isolated after removal of all fetus-derived tissues, followed by gentle scraping and blotting to remove the endometrial layer. Ovaries were dissociated from surrounding fat. Intact fetal lungs were harvested on ice. AF from each sac and lungs from each fetus were separately harvested for subsequent assignment of genotype. Maternal blood was collected at 18.5 dpc by retro-orbital puncture of anesthetized animals and allowed to clot for 2 hours at room temperature before centrifuging for 20 minutes at 3,000 *g*. Sera were harvested and stored at –80°C. All tissues were rinsed in ice-cold 1× PBS, flash frozen in liquid nitrogen, and stored at –80°C until analysis. Forelimbs from each fetus were placed in phenol-chloroform for DNA isolation and genotyping.

Animal surgery for injection of substances into AF. Timed-pregnant mice at 17.5 dpc were anesthetized with isoflurane via a precision vaporizer. The left uterine horn was gently pulled through a 1-cm incision made above the visible ovarian fat pad; SP-A (3.0 μg in 50 μl PBS), methylcarbamyl PAF-C-16 (Sigma-Aldrich, 0.25 ng in 50 μl PBS), or PBS (50 μl) was injected through the exposed uterine wall into each amniotic sac with a sterile 31-gauge half-inch needle (Becton Dickinson). The right uterine horn was untouched. The left uterine horn was returned to the abdominal cavity, the abdominal muscle wall was closed with Suturevet 4/0 polyglycolic acid synthetic absorbable sutures (Butler Schein Animal Health), and the skin was closed by using 7.5-mm wound clips (Perfect Agrafes Chirurgicales). The mice were kept on a warming pad and returned to their cages after recovery. One day later (18.5 dpc), mice were sacrificed, and myometrium, ovaries, and sera were harvested, as described above, or the mice were allowed to deliver for analysis of parturition timing.

Cell culture. Midgestation HFL tissues were obtained from Advanced Bioscience Resources. HFL type II pneumonocytes were isolated and cultured as described in detail previously (69). Briefly, the fetal lung tissues were minced and rinsed in serum-free Waymouth's MB752/1 medium (Invitrogen). Lung explants were placed on lens paper supported by stainless steel grids in 100-mm sterile dishes containing 3 ml serum-free Waymouth's medium containing Bt_2cAMP (1 mM) (Roche) for 3 to 5 days to enrich the population of differentiated type II cells. Cells were dispersed from the explants by digestion with collagenases type I (0.5 mg/ml; Sigma-Aldrich) and type IA (0.5 mg/ml; Sigma-Aldrich) for approximately 10 minutes. The resulting cell suspension was depleted of fibroblasts by incubation with diethylaminoethyl-dextran (250 μg/ml) for 30 minutes at 37°C, followed by centrifugation at 400 *g* for 5 minutes. The cell pellet was resuspended in Waymouth's MB752/1 medium containing 10% (vol/vol) FBS (Gemini Bio-Products), plated onto 6-well culture plates (1.5×10^6 cells per well) coated with extracellular matrix prepared from Madin-Darby

canine kidney cells (CRL 6253; ATCC) (69) and incubated overnight. Cultured cells were washed twice with medium to eliminate dead and nonadherent cells. Cells were then infected with lentiviruses containing shRNAs targeting SRC-1 and/or SRC-2 overnight and treated with or without Dex (10^{-7} M) in phenol red-free DMEM medium without FBS, with or without RU486. The human lung adenocarcinoma cell line A549 (CCL 185, ATCC) was maintained in Waymouth's MB752/1 medium containing FBS (10% vol/vol).

Lentivirus generation and infection. Lentiviral vectors containing shRNAs targeting SRC-1 or SRC-2 in pGIPZ vectors were obtained from a lentivirus shRNA library (Open Biosystems). Two different shRNA vectors were used for silencing SRC-1 (NCOA1, catalog RHS4430-99148018) and SRC-2 (NCOA2, catalog RHS4430-99141731), and their efficacy was validated. Lentiviral supernatants were produced in human embryonic kidney 293T (HEK 293T) cells by Polyethylenimine-mediated (Polysciences) transfection of plasmids pMD2.G, ps-PAX2, and human pGIPZ lentiviral shRNA for SRC-1 and SRC-2. Lentiviral supernatants were collected after 48 and 72 hours of culture. Viral titers were determined by measuring the coexpressed GFP after infection of HEK 293T cells.

HFL type II cells were then infected with recombinant lentiviruses containing shRNAs targeting SRC-1 and/or SRC-2 overnight and treated with Dex (10^{-7} M) in phenol red-free DMEM medium without FBS, in the absence or presence of RU486. For control experiments, cells were infected with nonsilencing pGIPZ lentiviral shRNA.

SP-A isolation. Human alveolar proteinosis lavage was delipidated using isopropyl ether and 1-butanol (6). Serum albumin was removed by extraction on a DEAE-Affigel blue gel column (Bio-Rad). Endotoxin was removed with polymyxin B agarose (Sigma-Aldrich). Remaining endotoxin content was assessed using a Limulus Amebocyte Lysate PYROGENT 06 Plus Assay Kit (Lonza). Purity of SP-A preparation was assessed by Coomassie blue staining and immunoblot analysis using an antibody raised against SP-A (70).

Quantitative RT-PCR. Total RNA from tissues or cells was extracted using an RNeasy Mini Kit (Qiagen). The purity and integrity of the RNA were checked spectroscopically and by gel electrophoresis before use. Quantification of total RNA was performed by measuring absorbance at OD_{260}. RNA was treated with DNase (Invitrogen) to remove any contaminating DNA, and 2 μg were reversed transcribed using the SuperScript III cDNA First-Strand Synthesis Kit (Invitrogen). Primer sets are listed in Supplemental Table 3. All primers were validated for efficiency by creating standard curves using a gradient of diluted samples with r^2 values larger than 0.96. The specificity of the primers was verified by examining the melting curve. Product purity was confirmed by gel electrophoresis. For quantitative analysis of mRNA, a CFX384 Real-Time PCR Detection System (Bio-Rad) was employed using Power SYBR Green PCR Master Mix (Applied Biosystems) for the detection of PCR products. The cycling conditions were 50°C for 2 minutes and 95°C for 10 minutes, followed by 45 cycles of 95°C for 15 seconds, and 60°C for 1 minute. As a negative control for all of the reactions, distilled water was used in place of cDNA. Amplification of the housekeeping gene *36B4* was determined for sample loading and normalization. Each sample was amplified in triplicate, and the mean of Cq value was calculated. The relative fold changes were calculated using the comparative Ct method ($2^{-\Delta\Delta Ct}$) (71).

Immunoblot analysis. Total protein extracts were prepared from tissues using RIPA buffer (Cell Signaling). Nuclear and cytoplasmic proteins were separated by NE-PER Nuclear and Cytoplasmic Extraction Reagents (Thermo Scientific). Equivalent amounts of protein determined by BCA assay (Thermo Scientific) were resolved by NuPAGE 4–12% Bis-Tris gel (Invitrogen) electrophoresis and blotted to Hybond-P PVDF membranes (Amersham Biosciences). The following primary antibodies and dilutions were used: anti–SP-A (1:500; ref. 70); anti-LPCAT1 (1:1,000; ab94903, Abcam); anti–SRC-1 (1:1,000; A300-344A, Bethyl Laboratories); anti–SRC-2 (1:1,000; A300-346A, Bethyl Laboratories); anti–NF-κB p65 (1:500; SC-372, Santa Cruz Biotechnology); anti–NF-κB p50 (1:500; SC-114, Santa Cruz Biotechnology); anti-CX43 (1:500; SC-6560-R, Santa Cruz Biotechnology); anti-OXTR (1:500; SC-33209, Santa Cruz Biotechnology); anti-AKR1B3 (1:500; SC-271007, Santa Cruz Biotechnology); anti-PGDH (1:500; SC-98907, Santa Cruz Biotechnology); anti–COX-2 (1:1,000; ab15191, Abcam); anti–20α-HSD (1:5,000; gift of Geula Gibori, University of Illinois, Chicago, Illinois, USA); anti-StAR (1:300; ab58013, Abcam); anti–β-actin (1:5,000; ab8227, Abcam); anti-GAPDH (1:2,000; ab9485, Abcam); and anti–histone H3 (1:2,000; 05-928, Millipore). Horseradish peroxidase–conjugated anti-rabbit or anti-mouse IgG (GE Healthcare) was used as secondary antibody. The membranes were developed using Supersignal West Pico Chemiluminescent substrate (Thermo Scientific). To control for sample loading and transfer, the ratio of band intensities to β-actin (for total protein; ab8227, Abcam), GAPDH (for cytoplasmic protein; ab9485, Abcam), or histone H3 (for nuclear protein; clone A3S 05-928, Millipore) was obtained to quantify the relative protein expression level.

Plasmid and siRNA transfection and luciferase assays. Various amounts of DNA flanking the transcription start site of the mouse *Lpcat1* gene were amplified from mouse genomic DNA and subcloned into the pGL4.12 vector (Promega) to generate luciferase reporter plasmids. Site-directed mutagenesis of putative GREs was performed using the QuikChange II Site-Directed Mutagenesis Kit (Agilent Technologies). All constructs and mutations were confirmed by DNA sequencing at the McDermott Center Sequencing Core, University of Texas Southwestern Medical Center. SRC-1 and SRC-2 transcripts in A549 cells were knocked-down by transfection of preannealed Silencer Select siRNA duplexes (s16461 for SRC-1 and/or s20528 for SRC-2, Ambion) using Lipofectamine RNAiMAX transfection reagent (Invitrogen). *Silencer* Negative Control #1 siRNA (AM4611, Ambion) was transfected as a negative control. The efficiency of knockdown was determined by RT-PCR and Western blotting. Twenty-four hours after transfection, WT, SRC-1, SRC-2, or SRC-1/-2 double-knockdown A549 cells were transfected with various *Lpcat1*-luciferase reporter constructs and Renilla luciferase plasmid using Lipofectamine 2000 transfection reagent (Invitrogen) according to the manufacturer's protocol. Dex (10^{-7} M) was added into the medium for 24 hours and then whole-cell lysates were prepared using Passive Lysis Buffer (Promega). Luciferase assays were performed using the Dual Luciferase Reporter Assay System (Promega), according to the manufacturer's protocol, in a GloMax plate-reading luminometer (Promega).

ChIP-qPCR. ChIP assays were performed on minced mouse fetal lung using a ChIP Assay Kit (Millipore) as described previously (72). Cross-linking was performed using formaldehyde (1% in PBS) at room temperature for 10 minutes with gentle rotation. The minced tissues were pelleted in a microfuge at full speed for 1 minute at 4°C. The pellets were washed, resuspended in SDS lysis buffer containing protease inhibitor cocktail, and then sonicated. Sheared chromatin was diluted in ChIP

dilution buffer and precleared according to the manufacturer's instructions. Precleared chromatin was incubated overnight with rabbit anti-GR monoclonal antibody (Cell Signaling, 12041), anti–SRC-1 (A300-344A, Bethyl Laboratories), anti–SRC-2 (A300-346A, Bethyl Laboratories), or rabbit IgG (Santa Cruz Biotechnology). After incubation for 1 hour on a rocking platform with Protein A Agarose Slurry/Salmon Sperm DNA (Sigma-Aldrich), the beads were washed following the manufacturer's instructions. Cross-linking was reversed by incubation in 1% SDS, 0.1 M $NaHCO_3$ at 65°C overnight. DNA was then extracted from samples using phenol/chloroform. Real-time qPCR was performed using Power SYBR Green PCR Master Mix and primer pairs for various regions of the *Lpcat1* promoter (listed in Supplemental Table 3).

Histological studies. Mouse ovaries were fixed in 4% paraformaldehyde, embedded in paraffin, and cut into 5-μm sections. Rabbit anti-StAR primary antibody (provided by Keith Parker, University of Texas Southwestern Medical Center) (73) was used at 1:100 dilution. Immunoreactivity using biotinylated secondary antibodies was detected with a Vectastain Elite ABC Kit (Vector Laboratories) and a Vector Nova Red Detection Kit (Vector Laboratories), using standard fixation and staining protocols (74).

$PGF_2\alpha$ and P_4 analysis. Myometrial and ovarian tissues were homogenized and $PGF_2\alpha$ levels were determined using an Enzyme Immunoassay (EIA) Kit (516011, Cayman Chemical) according to the manufacturer's protocol. $PGF_2\alpha$ levels were normalized to total protein. The levels of P_4 in serum were assayed using the EIA Kit (582601, Cayman Chemical) according to the manufacturer's protocol.

PAF analysis. AF from each sac was sonicated briefly on ice and then incubated with hyaluronidase (SEIKAGAKU Corp., 2 U/100 μl) for 10 minutes at 37°C to reduce viscosity. Fetal lungs were minced, homogenized on ice in 1× RIPA lysis buffer, sonicated briefly, and centrifuged; the supernatant was harvested for assay. PAF levels in AF and lung lysates were assayed using a competitive inhibition EIA Kit (E90526Mu, USCN Life Science Inc.) according to the manufacturer's instructions.

DPPC analysis. DPPC was analyzed using LC-MS (ABSciex QTRAP 4000 coupled to a Shimadzu LC20 HPLC). DPPC was resolved using a solvent gradient transitioning from 90% methanol to 100% methanol over 20 minutes. Both mobile phases contained 5 mM ammonium acetate. DPPC was measured using multiple reaction monitoring (MRM) in negative ion mode. The MRM for DPPC was 792.6; 255.3 Da d31-POPC (20 ng per sample, Avanti Polar Lipids) was added to each sample as an internal standard. Concentration was determined by comparing the intensity of the internal standard to a standard curve of DPPC (Avanti Polar Lipids).

Statistics. Data are expressed as mean ± SEM or as the mean percentage of control ± SEM. Differences between groups were analyzed by 1-way ANOVA, followed by Dunnett's multiple comparisons test, with statistical significance determined at the level of $P < 0.05$.

Study approval. All animal studies were approved by the Institutional Animal Care and Use Committee, University of Texas Southwestern Medical Center, and were in accordance with NIH guidelines. Midgestation HFL tissues were obtained from Advanced Bioscience Resources in accordance with the Donors Anatomical Gift Act of the State of Texas. The protocols were approved by the Institutional Review Board of University of Texas Southwestern Medical Center.

Acknowledgments

We thank Lei Wang for assistance with preparation of HFL type II cells, Mary Elhardt for breeding and genotyping the mice, Jo Smith for i.a. injections, and Zhida Su for assistance in creating recombinant lentiviruses expressing SRC-1 or SRC-2 shRNA. This work was supported by Prematurity Research Initiative grants 21-FY11-30 and 21-FY14-146 from the March of Dimes Foundation (to C.R. Mendelson) and NIH grants 5-P01-HD011149 and 5-R01-HL050022 (to C.R. Mendelson).

Address correspondence to: Carole R. Mendelson, Department of Biochemistry, University of Texas Southwestern Medical Center, 5323 Harry Hines Boulevard, Dallas, Texas 75390-9038, USA. Phone: 214.648.2944; E-mail: carole.mendelson@utsouthwestern.edu.

Lu Gao's present address is: Department of Physiology, Second Military Medical University, Shanghai, China.

Jennifer C. Condon's present address is: Department of Obstetrics-Gynecology, Wayne State University, Detroit, Michigan, USA.

Nora E. Renthal's present address is: Division of Endocrinology, Boston Children's Hospital, Harvard Medical School, Boston, Massachusetts, USA.

1. Blencowe H, et al. National, regional, and worldwide estimates of preterm birth rates in the year 2010 with time trends since 1990 for selected countries: a systematic analysis and implications. *Lancet*. 2012;379(9832):2162–2172.
2. Chang HH, et al. Preventing preterm births: analysis of trends and potential reductions with interventions in 39 countries with very high human development index. *Lancet*. 2013;381(9862):223–234.
3. Goldenberg RL, Culhane JF, Iams JD, Romero R. Epidemiology and causes of preterm birth. *Lancet*. 2008;371(9606):75–84.
4. Liu L, et al. Global, regional, and national causes of child mortality: an updated systematic analysis for 2010 with time trends since 2000. *Lancet*. 2012;379(9832):2151–2161.
5. Cox SM, Casey ML, MacDonald PC. Accumulation of interleukin-1β and interleukin-6 in amniotic fluid: a sequela of labour at term and preterm. *Hum Reprod Update*. 1997;3(5):517–527.
6. Condon JC, Jeyasuria P, Faust JM, Mendelson CR. Surfactant protein secreted by the maturing mouse fetal lung acts as a hormone that signals the initiation of parturition. *Proc Natl Acad Sci U S A*. 2004;101(14):4978–4983.
7. Osman I, et al. Leukocyte density and pro-inflammatory cytokine expression in human fetal membranes, decidua, cervix and myometrium before and during labour at term. *Mol Hum Reprod*. 2003;9(1):41–45.
8. Thomson AJ, et al. Leukocytes infiltrate the myometrium during human parturition: further evidence that labour is an inflammatory process. *Hum Reprod*. 1999;14(1):229–236.
9. Prince AL, Antony KM, Chu DM, Aagaard KM. The microbiome, parturition, and timing of birth: more questions than answers. *J Reprod Immunol*. 2014;104–105:12–19.
10. Romero R, Espinoza J, Goncalves LF, Kusanovic JP, Friel L, Hassan S. The role of inflammation and infection in preterm birth. *Semin Reprod Med*. 2007;25(1):21–39.
11. Mendelson CR. Minireview: fetal-maternal hormonal signaling in pregnancy and labor. *Mol Endocrinol*. 2009;23(7):947–954.
12. Sooranna SR, Lee Y, Kim LU, Mohan AR, Bennett PR, Johnson MR. Mechanical stretch activates type 2 cyclooxygenase via activator protein-1 transcription factor in human myometrial cells. *Mol Hum Reprod*. 2004;10(2):109–113.
13. Shynlova O, Tsui P, Dorogin A, Lye SJ. Monocyte chemoattractant protein-1 (CCL-2) integrates mechanical and endocrine signals that mediate term and preterm labor. *J Immunol*.

2008;181(2):1470–1479.
14. Challis JRG, Matthews SG, Gibb W, Lye SJ. Endocrine and paracrine regulation of birth at term and preterm. *Endocr Rev*. 2000;21(5):514–550.
15. Montalbano AP, Hawgood S, Mendelson CR. Mice deficient in surfactant protein A (SP-A) and SP-D or in TLR2 manifest delayed parturition and decreased expression of inflammatory and contractile genes. *Endocrinology*. 2013;154(1):483–498.
16. Shaw G, Renfree MB. Fetal control of parturition in marsupials. *Reprod Fertil Dev*. 2001; 13(7–8):653–659.
17. Lopez BA, Newman GE, Phizackerley PJ, Turnbull AC. Surfactant stimulates prostaglandin E production in human amnion. *Br J Obstet Gynaecol*. 1988;95(10):1013–1017.
18. Alcorn JL, et al. Analysis of genomic regions involved in regulation of the rabbit surfactant protein A gene in transgenic mice. *Am J Physiol*. 1999;277(2:Pt 1):L349–L361.
19. Liu D, Yi M, Smith ME, Mendelson CR. TTF-1 response element is critical for temporal and spatial regulation and necessary for hormonal regulation of human surfactant protein-A2 promoter activity. *Am J Physiol Lung Cell Mol Physiol*. 2008;295(2):L264–L271.
20. Liu D, Benlhabib H, Mendelson CR. cAMP enhances estrogen-related receptor α (ERRα) transcriptional activity at the SP-A promoter by increasing its interaction with protein kinase A and steroid receptor coactivator 2 (SRC-2). *Mol Endocrinol*. 2009;23(6):772–783.
21. Yi M, Tong GX, Murry B, Mendelson CR. Role of CBP/p300 and SRC-1 in transcriptional regulation of the pulmonary surfactant protein-A (SP-A) gene by thyroid transcription factor-1 (TTF-1). *J Biol Chem*. 2001;277(4):2997–3005.
22. Islam KN, Mendelson CR. Permissive effects of oxygen on cyclic AMP and interleukin-1 stimulation of surfactant protein A gene expression are mediated by epigenetic mechanisms. *Mol Cell Biol*. 2006;26(8):2901–2912.
23. Lonard DM, O'Malley BW. The expanding cosmos of nuclear receptor coactivators. *Cell*. 2006;125(3):411–414.
24. Xu J, Wu RC, O'Malley BW. Normal and cancer-related functions of the p160 steroid receptor co-activator (SRC) family. *Nat Rev Cancer*. 2009;9(9):615–630.
25. Johnson AB, O'Malley BW. Steroid receptor coactivators 1, 2, and 3: critical regulators of nuclear receptor activity and steroid receptor modulator (SRM)-based cancer therapy. *Mol Cell Endocrinol*. 2012;348(2):430–439.
26. Xu J, Qiu Y, DeMayo FJ, Tsai SY, Tsai MJ, O'Malley BW. Partial hormone resistance in mice with disruption of the steroid receptor coactivator-1 (SRC-1) gene. *Science*. 1998;279(5358):1922–1925.
27. Ye X, et al. Roles of steroid receptor coactivator (SRC)-1 and transcriptional intermediary factor (TIF) 2 in androgen receptor activity in mice. *Proc Natl Acad Sci U S A*. 2005;102(27):9487–9492.
28. Gehin M, Mark M, Dennefeld C, Dierich A, Gronemeyer H, Chambon P. The function of TIF2/GRIP1 in mouse reproduction is distinct from those of SRC-1 and p/CIP. *Mol Cell Biol*. 2002;22(16):5923–5937.
29. Mark M, et al. Partially redundant functions of SRC-1 and TIF2 in postnatal survival and male reproduction. *Proc Natl Acad Sci U S A*. 2004;101(13):4453–4458.
30. Weaver TE, Conkright JJ. Function of surfactant proteins B and C. *Annu Rev Physiol*. 2001;63:555–578.
31. Whitsett JA, Weaver TE. Hydrophobic surfactant proteins in lung function and disease. *N Engl J Med*. 2002;347(26):2141–2148.
32. Besnard V, et al. Conditional deletion of Abca3 in alveolar type II cells alters surfactant homeostasis in newborn and adult mice. *Am J Physiol Lung Cell Mol Physiol*. 2010;298(5):L646–L659.
33. Cheong N, et al. ABCA3 is critical for lamellar body biogenesis in vivo. *J Biol Chem*. 2007;282(33):23811–23817.
34. Hardy DB, Janowski BA, Corey DR, Mendelson CR. Progesterone receptor (PR) plays a major anti-inflammatory role in human myometrial cells by antagonism of NF-κB activation of cyclooxygenase 2 (COX-2) expression. *Mol Endocrinol*. 2006;20(11):2724–2733.
35. Soloff MS, Izban MG, Cook DL Jr, Jeng YJ, Mifflin RC. Interleukin-1-induced NF-κB recruitment to the oxytocin receptor gene inhibits RNA polymerase II-promoter interactions in cultured human myometrial cells. *Mol Hum Reprod*. 2006;12(10):619–624.
36. Stocco C, Telleria C, Gibori G. The molecular control of corpus luteum formation, function, and regression. *Endocr Rev*. 2007;28(1):117–149.
37. Niswender GD, Juengel JL, Silva PJ, Rollyson MK, McIntush EW. Mechanisms controlling the function and life span of the corpus luteum. *Physiol Rev*. 2000;80(1):1–29.
38. Clark BJ, Wells J, King SR, Stocco DM. The purification, cloning, and expression of a novel luteinizing hormone-induced mitochondrial protein in MA-10 mouse Leydig tumor cells. Characterization of the steroidogenic acute regulatory protein (StAR). *J Biol Chem*. 1994;269(45):28314–28322.
39. Lin D, et al. Role of steroidogenic acute regulatory protein in adrenal and gonadal steroidogenesis. *Science*. 1995;267(5205):1828–1831.
40. Fiedler EP, Plouffe L Jr, Hales DB, Hales KH, Khan I. Prostaglandin (F2α) induces a rapid decline in progesterone production and steroidogenic acute regulatory protein expression in isolated rat corpus luteum without altering messenger ribonucleic acid expression. *Biol Reprod*. 1999;61(3):643–650.
41. Williams KC, Renthal NE, Condon JC, Gerard RD, Mendelson CR. MicroRNA-200a serves a key role in the decline of progesterone receptor function leading to term and preterm labor. *Proc Natl Acad Sci U S A*. 2012;109(19):7529–7534.
42. Bridges JP, Ikegami M, Brilli LL, Chen X, Mason RJ, Shannon JM. LPCAT1 regulates surfactant phospholipid synthesis and is required for transitioning to air breathing in mice. *J Clin Invest*. 2010;120(5):1736–1748.
43. Chen X, Hyatt BA, Mucenski ML, Mason RJ, Shannon JM. Identification and characterization of a lysophosphatidylcholine acyltransferase in alveolar type II cells. *Proc Natl Acad Sci U S A*. 2006;103(31):11724–11729.
44. Nakanishi H, et al. Cloning and characterization of mouse lung-type acyl-CoA:lysophosphatidylcholine acyltransferase 1 (LPCAT1). Expression in alveolar type II cells and possible involvement in surfactant production. *J Biol Chem*. 2006;281(29):20140–20147.
45. Harayama T, Shindou H, Ogasawara R, Suwabe A, Shimizu T. Identification of a novel noninflammatory biosynthetic pathway of platelet-activating factor. *J Biol Chem*. 2008;283(17):11097–11106.
46. Frenkel RA, Muguruma K, Johnston JM. The biochemical role of platelet-activating factor in reproduction. *Prog Lipid Res*. 1996;35(2):155–168.
47. Hoffman DR, Romero R, Johnston JM. Detection of platelet-activating factor in amniotic fluid of complicated pregnancies. *Am J Obstet Gynecol*. 1990;162(2):525–528.
48. Toyoshima K, Narahara H, Furukawa M, Frenkel RA, Johnston JM. Platelet-activating factor. Role in fetal lung development and relationship to normal and premature labor. *Clin Perinatol*. 1995;22(2):263–280.
49. Yasuda K, Furukawa M, Johnston JM. Effect of estrogens on plasma platelet-activating factor acetylhydrolase and the timing of parturition in the rat. *Biol Reprod*. 1996;54(1):224–229.
50. Zhu YP, Hoffman DR, Hwang SB, Miyaura S, Johnston JM. Prolongation of parturition in the pregnant rat following treatment with a platelet activating factor receptor antagonist. *Biol Reprod*. 1991;44(1):39–42.
51. Butler PL, Mallampalli RK. Cross-talk between remodeling and de novo pathways maintains phospholipid balance through ubiquitination. *J Biol Chem*. 2010;285(9):6246–6258.
52. Morita M, Imanaka T. Peroxisomal ABC transporters: structure, function and role in disease. *Biochim Biophys Acta*. 2012;1822(9):1387–1396.
53. Maul H, Shi L, Marx SG, Garfield RE, Saade GR. Local application of platelet-activating factor induces cervical ripening accompanied by infiltration of polymorphonuclear leukocytes in rats. *Am J Obstet Gynecol*. 2002;187(4):829–833.
54. Sugano T, Nasu K, Narahara H, Kawano Y, Nishida Y, Miyakawa I. Platelet-activating factor induces an imbalance between matrix metalloproteinase-1 and tissue inhibitor of metalloproteinases-1 expression in human uterine cervical fibroblasts. *Biol Reprod*. 2000;62(3):540–546.
55. Sugano T, Narahara H, Nasu K, Arima K, Fujisawa K, Miyakawa I. Effects of platelet-activating factor on cytokine production by human uterine cervical fibroblasts. *Mol Hum Reprod*. 2001;7(5):475–481.
56. Ishii S, et al. Impaired anaphylactic responses with intact sensitivity to endotoxin in mice lacking a platelet-activating factor receptor. *J Exp Med*. 1998;187(11):1779–1788.
57. Jeanneton O, Delvaux M, Botella A, Frexinos J, Bueno L. Platelet-activating factor (PAF) induces a contraction of isolated smooth muscle cells from guinea pig ileum: intracellular pathway involved. *J Pharmacol Exp Ther*. 1993;267(1):31–37.
58. Kim BK, Ozaki H, Lee SM, Karaki H. Increased sensitivity of rat myometrium to the contractile effect of platelet activating factor before delivery. *Br J Pharmacol*. 1995;115(7):1211–1214.
59. Montrucchio G, Alloatti G, Tetta C, Roffinello C, Emanuelli G, Camussi G. In vitro contractile effect of platelet-activating factor on guinea-pig myo-

metrium. *Prostaglandins*. 1986;32(4):539–554.
60. Tetta C, et al. Platelet-activating factor contracts human myometrium in vitro. *Proc Soc Exp Biol Med*. 1986;183(3):376–381.
61. Silver RK, Caplan MS, Kelly AM. Amniotic fluid platelet-activating factor (PAF) is elevated in patients with tocolytic failure and preterm delivery. *Prostaglandins*. 1992;43(2):181–187.
62. Winnay JN, Xu J, O'Malley BW, Hammer GD. Steroid receptor coactivator-1-deficient mice exhibit altered hypothalamic-pituitary-adrenal axis function. *Endocrinology*. 2006;147(3):1322–1332.
63. Bird AD, Choo YL, Hooper SB, McDougall AR, Cole TJ. Mesenchymal glucocorticoid receptor regulates the development of multiple cell layers of the mouse lung. *Am J Respir Cell Mol Biol*. 2014;50(2):419–428.
64. Cole TJ, et al. Targeted disruption of the glucocorticoid receptor gene blocks adrenergic chromaffin cell development and severely retards lung maturation. *Genes Dev*. 1995;9(13):1608–1621.
65. Habermehl D, et al. Glucocorticoid activity during lung maturation is essential in mesenchymal and less in alveolar epithelial cells. *Mol Endocrinol*. 2011;25(8):1280–1288.
66. Kapoor A, Petropoulos S, Matthews SG. Fetal programming of hypothalamic-pituitary-adrenal (HPA) axis function and behavior by synthetic glucocorticoids. *Brain Res Rev*. 2008;57(2):586–595.
67. Liggins GC, Howie RN. A controlled trial of antepartum glucocorticoid treatment for prevention of the respiratory distress syndrome in premature infants. *Pediatrics*. 1972;50(4):515–525.
68. Rooney SA, Young SL, Mendelson CR. Molecular and cellular processing of lung surfactant. *FASEB J*. 1994;8(12):957–967.
69. Alcorn JL, Smith ME, Smith JF, Margraf LR, Mendelson CR. Primary cell culture of human type II pneumonocytes: maintenance of a differentiated phenotype and transfection with recombinant adenoviruses. *Am J Respir Cell Mol Biol*. 1997;17(6):672–682.
70. Odom MJ, Snyder JM, Mendelson CR. Adenosine 3′,5′-monophosphate analogs and β-adrenergic agonists induce the synthesis of the major surfactant apoprotein in human fetal lung in vitro. *Endocrinology*. 1987;121(3):1155–1163.
71. Livak KJ, Schmittgen TD. Analysis of relative gene expression data using real-time quantitative PCR and the 2(-Delta Delta C(T)) Method. *Methods*. 2001;25(4):402–408.
72. Benlhabib H, Mendelson CR. Epigenetic regulation of surfactant protein A gene (SP-A) expression in fetal lung reveals a critical role for Suv39h methyltransferases during development and hypoxia. *Mol Cell Biol*. 2011;31(10):1949–1958.
73. King SR, et al. An essential component in steroid synthesis, the steroidogenic acute regulatory protein, is expressed in discrete regions of the brain. *J Neurosci*. 2002;22(24):10613–10620.
74. Condon JC, Jeyasuria P, Faust JM, Wilson JM, Mendelson CR. A decline in progesterone receptor coactivators in the pregnant uterus at term may antagonize progesterone receptor function and contribute to the initiation of labor. *Proc Natl Acad Sci U S A*. 2003;100(16):9518–9523.